Pergamon

Geochimica et Cosmochimica Acta, Vol. 67, No. 19, pp. 3625–3644, 2003

0016-7037/03 $30.00 + .00

doi:10.1016/S0016-7037(03)00136-4

Experimental constraints on the hydrothermal reactivity of organic acids and acid anions: I. Formic acid and formate

THOMAS M. MCCOLLOM* and JEFFREY S. SEEWALD
Woods Hole Oceanographic Institution, MS #4, Woods Hole, MA 02543, USA

(*Received June* 12, 2002; revised 30 January 2003; *accepted in revised form January* 30, 2003)

Abstract—A series of hydrothermal experiments covering a range of temperatures from 175 to 260°C examined the decomposition of formic acid and formate and also investigated the production of formate from reduction of CO_2. Decomposition rates measured in this study, which were conducted in gold-TiO_2 reactors, were several orders of magnitude slower than those reported in previous studies conducted in steel and Ti-metal reactors, indicating the previous studies substantially overestimated the rate of the reaction owing to reactor catalysis. Although experiments were conducted with several different minerals present (hematite, magnetite, serpentinized olivine, NiFe-alloy), the decomposition rates were similar in each experiment once the effects of fluid pH were accounted for, suggesting that the minerals had no effect on the stability of formic acid or formate. At higher temperatures (>225°C), the rates of both the decomposition of formate and the reduction of CO_2 to formate were sufficiently rapid that reactions between dissolved CO_2 and formate rapidly attained a state of metastable thermodynamic equilibrium. The results suggest that the amount of formate in many subsurface and hydrothermal fluids is likely to be controlled by equilibrium with dissolved CO_2 at the prevailing oxidation state and pH of the fluid. This may account for the high concentrations of formate observed in strongly reducing environments such as serpentinites, as well as the low concentrations relative to other organic acid anions in mildly reducing environments such as oil-filed brines and formation waters in sedimentary basins. Although formate has been suggested to be a reaction intermediate in the formation of abiotic hydrocarbons from reduction of aqueous CO_2, production of hydrocarbons was not observed in any of the experiments, except for trace amounts of methane, despite high concentrations of formate and strongly reducing conditions. *Copyright © 2003 Elsevier Ltd*

1. INTRODUCTION

Short-chain organic acids and acid anions frequently represent a large fraction of the total dissolved organic carbon in aqueous geologic fluids. Collectively, organic acid and acid anions have been proposed to have a significant role in a variety of geochemical processes, including the formation of oil and natural gas deposits, transportation of metals in ore-forming solution, enhancing porosity in sedimentary basins, and providing food for microbes in subsurface habitats (see reviews in Pittman and Lewan, 1994). Formic acid (HCOOH) and its conjugate base, formate ($HCOO^-$), can be considered as the simplest of the organic acids and acid anions that occur in natural waters. Formate[1] has been reported to occur along with acetate and other organic acid anions in a wide variety of geologic environments, including formation waters from sedimentary basins, oil-field brines, natural spring waters, pore waters from seafloor serpentinites, and hydrothermal fluids (Fisher and Boles, 1990; MacGowan and Surdam, 1990; Martens, 1990; Barth, 1991; Haggerty, 1991; Haggerty and Fisher, 1992; Kawamura and Nissenbaum, 1992; Amend et al., 1998; Zeng and Liu, 2001). Formate is generated in laboratory experiments designed to simulate the thermal maturation of organic matter (Lundegard and Sentfle, 1987; Kharaka et al., 1993; Shebl and Surdam, 1996), and has been suggested to be a reaction intermediate in the abiotic reduction of aqueous CO_2 to methane and other hydrocarbons (Horita and Berndt, 1999; Schoonen et al., 1999).

By analogy with other organic acid and acid anions, formic acid and formate are thought to be generated during thermal maturation of organic matter and to subsequently decompose during continued thermal stress (see Pittman and Lewan, 1994). As such, formate and other organic acids can be viewed as reaction intermediates in the decomposition of complex organic matter to CO_2, CH_4, and other light hydrocarbons. In most geologic fluids, the abundance of formate is much lower than the abundances of coexisting acetate and propionate, which has been attributed to a faster decomposition rate for formate compared to other acid anions. However, in some cases, such as hydrothermal fluids, pore fluids from serpentinites, and the aqueous products of hydrous pyrolysis of kerogens, the abundance of formate is comparable to, or greater than, acetate and propionate (e.g., Martens, 1990; Haggerty, 1991; Haggerty and Fisher, 1992; Shebl and Surdam, 1996; Amend et al., 1998; Zeng and Liu, 2001). The higher relative abundance of formate in these instances has been attributed to sampling of the fluids soon after the acids formed and before the formate had sufficient time to decompose (e.g., Haggerty, 1991; Bell and Palmer, 1994).

* Author to whom correspondence should be addressed, at the Laboratory for Atmospheric and Space Physics, Campus Box 392, University of Colorado, Boulder, CO 80309-0392, USA (mccollom@lasp.colorado.edu).

1 In natural samples, organic acids and acid anions are generally analyzed and reported together in anion form. Consequently, reported concentrations of formate, acetate, etc. may include both organic acids and acid anions. For convenience, formate will be used in this report to refer to formic acid and formate collectively when the exact speciation is uncertain or not germane to the discussion. Similarly, ΣCO_2 will be used to refer to all dissolved CO_2 species collectively, including $CO_{2(aq)}$, HCO_3^-, and CO_3^{2-}.

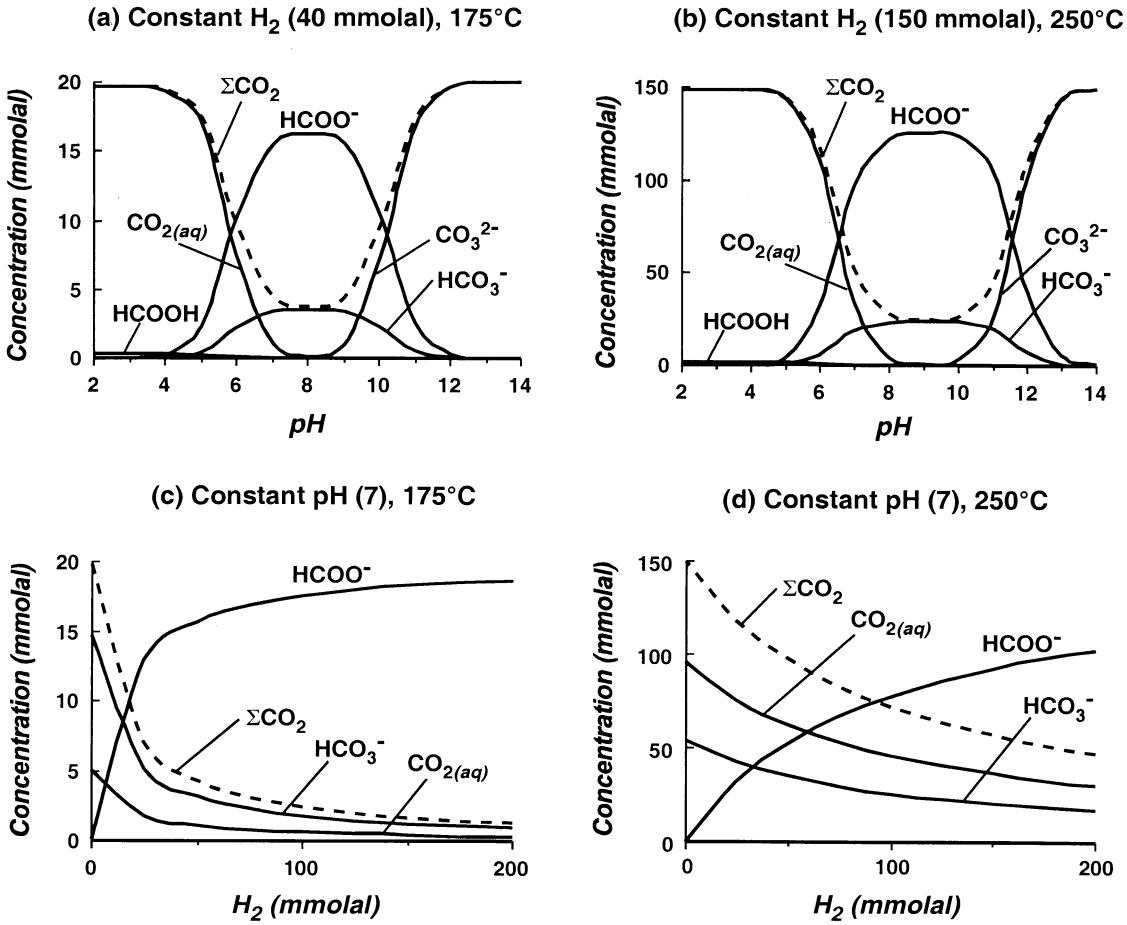

Fig. 1. Calculated equilibrium distribution of $CO_{2(aq)}$, HCO_3^-, CO_3^{2-}, $HCOOH_{(aq)}$, and $HCOO^-$ at 175 and 250°C, 350 bars. Equilibrium speciation as a function of pH for constant $H_{2(aq)}$ concentration is shown in (a) and (b), while (c) and (d) show the speciation as a function of H_2(aq) concentration at a constant pH of 7. Figures (a) and (c) are calculated for a total dissolved carbon concentration of 20 mmolal, while (b) and (d) are calculated for a total dissolved carbon concentration of 150 mmolal. The figures represent metastable equilibrium distributions since most of the carbon would be present in the form of CH_4 at stable equilibrium for the reducing conditions shown in the figures.

There are two principal pathways for decomposition of formic acid, which are generally referred to as decarboxylation and dehydration:

$$HCOOH = CO_2 + H_2 \ (decarboxylation) \quad (1)$$

$$HCOOH = CO + H_2O \ (dehydration) \quad (2)$$

When formic acid is dissolved in water, the decarboxylation pathway strongly predominates, while dehydration is favored in the gas phase (Bjerre and Sørenson, 1992; Akiya and Savage, 1998; Maiella and Brill, 1998; Yu and Savage, 1998). Analogous reactions for formate can be written as

$$HCOO^- + H_2O = HCO_3^- + H_2 \quad (3)$$

$$HCOO^- + H^+ = CO_2 + H_2 \quad (4)$$

$$HCOO^- + H^+ = CO + H_2. \quad (5)$$

These reactions are reversible, so that formic acid and formate can be generated by reduction of dissolved CO_2 or HCO_3^-, or by hydration of CO, as the reactions proceed from right to left as written.

Recently, McCollom and Seewald (2001) reported that both the decarboxylation of formate and the reduction of dissolved HCO_3^- to formate was sufficiently rapid at 300°C that a state of chemical thermodynamic equilibrium was established between these compounds in $<$ 24 h. This result suggested that the abundance of formate in many geologic fluids might be controlled by thermodynamic equilibrium rather than kinetic factors. The abundances of formate and formic acid in chemical equilibrium with dissolved CO_2 species are strongly dependent on pH and oxidation state (Fig. 1). For all values of pH, more strongly reducing conditions increase the proportions of formic acid and formate in equilibrium with ΣCO_2. Nevertheless, equilibrium concentrations of formic acid and formate are small at low pH, even under very strongly reducing conditions. At moderately alkaline pH values, the thermodynamic stability of formate increases relative to dissolved ΣCO_2 and the proportion of formate at equilibrium increases substantially. Under

reducing conditions and alkaline pH, formate can make up a large fraction of the total dissolved carbon at equilibrium (Fig. 1). It must be noted that the relative proportions of ΣCO_2 and formate under reducing conditions shown in Figure 1 represents a metastable equilibrium, since most of the dissolved carbon would be converted to CH_4 if stable thermodynamic equilibrium for the overall system were attained. However, formation of CH_4 from reduction of dissolved CO_2 or formate is kinetically inhibited under hydrothermal conditions unless specific catalysts are present (McCollom and Seewald, 2001).

At present, there are few experimental data available on the reactivity of formic acid and formate in aqueous solution. For the most part, the available data are limited to high temperatures (>300°C) and low water densities (Bjerre and Sørenson, 1992; Akiya and Savage, 1998; Maiella and Brill, 1998; Yu and Savage, 1998). Furthermore, nearly all previous studies were conducted in steel or Ti-metal vessels where interactions with the reactor walls apparently accelerated reaction rates (Bjerre and Sørenson, 1992; Maiella and Brill, 1998). Consequently, the reactivities of aqueous formic acid and formate in geologic environments remain largely unknown.

Presented here are results of laboratory experiments performed to investigate the formation and decomposition of formic acid and formate under hydrothermal conditions. In particular, the experiments were designed to address the following issues: (1) the effect of temperature and pH on reaction rates for decomposition of formic acid and formate and for the production of formate from reduction of CO_2, (2) the potential for equilibration between formate and dissolved ΣCO_2, (3) the potential for reduction of dissolved CO_2 to methane and other hydrocarbons under hydrothermal conditions and the role of formate in the process, and (4) the impact of mineral surfaces on reactions involving formic acid and formate. This is the first of two reports presenting results from hydrothermal experiments with organic acids. A companion paper examines the reactivities of acetic acid, acetate, and valeric acid (*n*-pentanoic acid) (McCollom and Seewald, 2003).

2. METHODS

All experiments were conducted in a flexible-cell hydrothermal apparatus (Fig. 2; Seyfried et al., 1987). The internal reaction cell consisted of a flexible gold bag with titanium fittings. This reaction cell was confined within a stainless steel pressure housing using H_2O as the pressurizing fluid. Because the flexible reaction cell collapses or expands as fluid is removed or added, the experiments could be conducted at constant pressure with no vapor phase present. The sampling valve was attached to the reaction cell with a capillary tube. This valve allowed samples of the fluid to be obtained during the course of the experiments, and also allowed additional reactants to be periodically injected into the reaction cell. The titanium fittings were combusted in air for 24 h at 400°C before use in the experiment to form an inert TiO_2 layer on the surface. All experiments were conducted at a pressure of 350 bars.

The experiments were conducted by injecting aqueous solutions of HCOOH or $NaHCO_3$ into the reaction cell, followed by removal of fluid samples through the valve to follow the progress of reactions over time. For most injections, ^{13}C-labeled reactants were used (99% $H^{13}COOH$ or $NaH^{13}CO_3$; Cambridge Isotope Labs) to provide a tracer for injected carbon. In some cases, NaOH and $MgCl_2$ were also injected to adjust fluid pH. Several different minerals were included in separate experiments. The intent of including the minerals was two-fold: first, to provide reducing conditions within the reaction cell through reaction of the minerals with water and, second, to provide potential catalytic surfaces similar to those that occur in sedimentary basins and hydrothermal environments. In each experiment, the minerals were heated with water before injection of HCOOH or $NaHCO_3$ to allow reducing conditions to develop before introducing the reactants. The initial heating period also made it possible to evaluate background levels of CO_2 and organic compounds generated from the minerals.

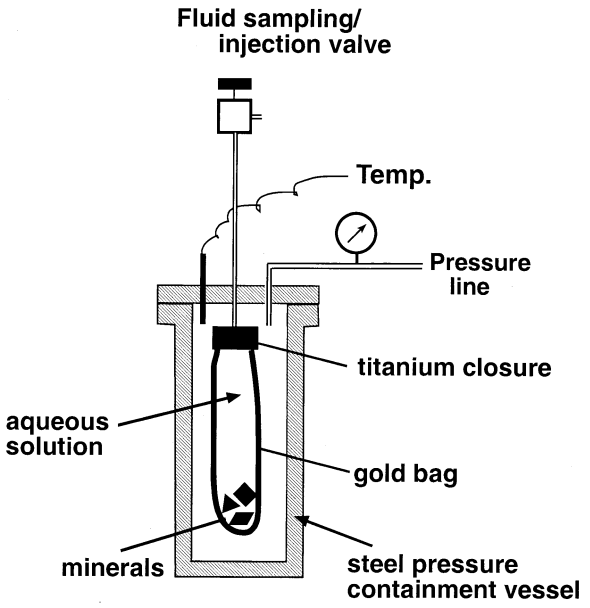

Fig. 2. Schematic drawing of the flexible-cell hydrothermal apparatus used in the laboratory experiments.

Solids included in separate experiments included: (1) nickel-iron powder, (2) powdered olivine, or (3) hematite plus magnetite. The nickel-iron powder had a composition of 42 wt.% Ni and 58 wt.% Fe and had a reported purity of > 99% on a metals basis (Johnson Matthey). The olivine was obtained from Excalibur Minerals (Peekskill, NY) and consisted of crystals (~30–80 mm diameter) that were hand-picked from mantle peridotite xenoliths originating from San Carlos, AZ. The composition of the olivine, as determined by electron microprobe, is given in Table 1. To avoid contamination with organic solvents, the crystals were washed only with Milli-Q water. After drying, the olivine was crushed to a fine powder for use in the experiments. The hematite and magnetite were finely powdered synthetic minerals (Alfa Aesar).

Separate fluid samples were taken directly into glass/Teflon gas-tight syringes (0.2–0.5 g each) and were used to analyze: (1) dissolved H_2, (2) dissolved CO_2, CH_4, and C_2-C_6 hydrocarbons, (3) cations and anions, including formate and other carboxylic acid anions. Concentrations of total dissolved CO_2 (ΣCO_2), CH_4, and C_2-C_6 hydrocarbons were determined by gas chromatography (GC) following extraction from an acidified fluid sample using a purge-and-trap device. Dissolved H_2 was analyzed by GC following a headspace extraction of the sample

Table 1. Composition of San Carlos olivine used in the experiment.

Oxide	Weight percent
SiO_2	40.31
TiO_2	0.01
Al_2O_3	0.01
Cr_2O_3	0.03
FeO	9.53
MgO	49.74
CaO	0.06
NiO	0.32

syringe with N_2. Gas chromatography-mass spectrometry (GCMS) was used on selected samples to determine the extent to which carbon derived from isotopically labeled reactants was incorporated into aqueous reaction products. Cations and anions, including organic acids, were analyzed by ion chromatography. Organic acids and their conjugate bases were measured in anion form and are reported as a total (e.g., Σformate = $HCOOH_{(aq)} + HCOO^-$). In most cases, the concentrations reported in the tables represent averages for analyses of two separate fluid samples. Estimated analytical uncertainty for all compounds is $\pm$5%. Trace amounts of C_4-C_6 hydrocarbons as well as benzene and toluene were observed throughout the experiments. However, because these compounds were always present at very low levels and appeared to derive exclusively from background sources rather than reactions involving the compounds under study, their concentrations are not reported in detail. C_3-C_5 carboxylic acids were below detection limits ($<$0.1 mmol kg^{-1}) in all experiments.

Thermodynamic calculations were used to determine equilibrium distributions of aqueous species and to estimate in situ pH. The required thermodynamic data for these calculations were generated using the computer program SUPCRT92 (Johnson et al., 1992) with additional data from Shock (1995). In situ pH values were calculated from mass and charge balance using Na, Mg, Ca, Cl, H_2, and total dissolved carbon as input constraints. The calculations were performed using the computer program EQ3NR, which takes into account the formation of aqueous complexes, activity coefficients, and carbon speciation in determination of pH (Wolery, 1992). In those cases where measurable concentrations of Mg were observed, the calculated pH was also constrained by the measured Mg concentrations and equilibrium constants for saturation of the fluid with the minerals brucite or magnesite as appropriate:

$$Mg^{2+} + 2H_2O = \underset{\text{Brucite}}{Mg(OH)_2} + 2H^+ \quad (6)$$

$$Mg^{2+} + HCO_3^- = \underset{\text{Magnesite}}{MgCO_3} + H^+. \quad (7)$$

3. RESULTS

3.1. Reactions in the Presence of NiFe Alloy Plus Magnetite

The experiment was initiated by heating nickel-iron powder ($NiFe_{1.4}$) with liquid H_2O at 335°C for 470 h. Examination of the solids by XRD and electron microprobe after the termination of the experiment indicated that reaction of the powder with water led to the formation of magnetite and a NiFe alloy containing 2 to 9 mol.% Fe. This process can be approximated by the reaction

$$NiFe_{1.4} + 1.8H_2O = \underset{\text{alloy}}{NiFe_{0.05}} + \underset{\text{magnetite}}{0.45Fe_3O_4} + 1.8H_{2(aq)}. \quad (8)$$

The production of dissolved H_2 by this reaction resulted in strongly reducing conditions within the reaction vessel. At 424 h, the measured H_2 concentration had increased to 119 mmol kg^{-1} (Table 2).

After 470 h at 330°C, the temperature of the experiment was lowered to 177°C and a solution of ^{13}C-labeled formic acid (99% $H^{13}COOH$) was injected into the reaction cell to attain a Σformate concentration of 230 mmol kg^{-1}. Over the next 700 h, the measured Σformate concentration decreased steadily by ~50 mmol kg^{-1} while the H_2 concentration increased by a similar amount, indicating partial decomposition of the injected formic acid by decarboxylation (Fig. 3a; Table 2). The ΣCO_2 concentration initially increased and then remained essentially constant during this period. The absence of aqueous ΣCO_2 increases during formic acid decomposition suggests CO_2 may have been removed from solution along with some H_2 by precipitation of iron carbonate (siderite; $FeCO_3$) according to the reaction:

$$\underset{\text{Magnetite}}{Fe_3O_4} + 3CO_{2(aq)} + H_{2(aq)} = \underset{\text{Siderite}}{3FeCO_3} + H_2O. \quad (9)$$

Thermodynamic calculations were performed to determine whether the formic acid decomposition had led to equilibrium between ΣCO_2 and Σformate. Comparison of the measured $\Sigma CO_2/\Sigma$formate ratio with the ratio expected for equilibration between ΣCO_2 and Σformate at the calculated in situ pH and measured H_2 concentration indicates that the reaction was progressing towards equilibrium, yet remained far from equilibrium after nearly 700 h at 177°C (Fig. 3b).

At 1171 h, the effect of higher temperature on formic acid decomposition was assessed by raising the temperature to 260°C and injecting additional HCOOH to a final concentration of 257 mmol kg^{-1}. Within 91 h, nearly all of the injected formic acid had decomposed, resulting in sharply increased concentrations of ΣCO_2 and H_2 (Fig. 4a). After this initial rapid reaction, the measured concentrations of H_2, ΣCO_2, and Σformate remained essentially constant for the next 2000 h. The measured $\Sigma CO_2/\Sigma$formate ratio 91 h after the injection was nearly identical to the calculated equilibrium ratio for the measured H_2 concentration and the estimated in situ pH of ~4.4 (Fig. 4b), suggesting that the system rapidly attained equilibrium between ΣCO_2 and Σformate at this temperature. The constant concentrations over the succeeding 2000 h reflect steady state conditions once equilibrium was achieved.

For equilibrium at the relatively reducing conditions present in the reaction vessel, an increase in pH from acidic to mildly alkaline conditions at a constant temperature of 260°C should result in a reduction of dissolved ΣCO_2 to formate (Fig. 1). Accordingly, a solution of NaOH was injected into the experiment at 3265 h to raise the pH and observe the rate of ΣCO_2 conversion to formate. Magnesium chloride was also included in the injection to provide a tracer to monitor in situ pH through precipitation of magnesite (Eqn. 7).

The increase in pH resulted in rapid conversion of H_2 and ΣCO_2 to Σformate, with $>$ 50 mmol kg^{-1} of Σformate produced within 40 h after the injection (Fig. 4a). Continued heating for $>$ 800 additional hours, however, generated no further increase in the measured Σformate concentration despite continued high concentrations of H_2 and ΣCO_2. The concentrations of ΣCO_2 and H_2 decreased slightly during this period, presumably owing to further precipitation of Fe and Mg carbonates. As shown in Figure 4b, comparison of measured and equilibrium $\Sigma CO_2/\Sigma$formate ratios indicates that reduction of ΣCO_2 to Σformate had apparently attained equilibrium within 40 h after the pH was raised.

The temperature of the experiment was lowered to 175°C at 4217 h and, after 90 h at this temperature, a solution of NaCl and additional $H^{13}COOH$ was injected to determine whether the salinity of the fluid would have any appreciable affect on the rate of formic acid decomposition. An increase in Mg concentration was observed following the injection, reflecting partial dissolution of magnesite in response to a decrease in the

Table 2. Fluid composition during reaction of aqueous solutions with NiFe alloy.

Time (h)	ΔTime[a] (h)	H_2 (m)	ΣCO_2 (m)	ΣFormate (m)	CH_4 (m)	C_2H_4 (μ)	C_2H_6 (μ)	C_3H_6 (μ)	C_3H_8 (μ)	ΣAcetate (m)	CH_3OH (m)	Cl (m)	Na (m)	Mg (m)	$\%^{13}C$ ΣCO_2	$\%^{13}C$ CH_4	Fluid[b] (g)	Calc. pH[c]
0					*Start of experiment; initial temperature = 335°C*													
424	—	119	0.12	—	1.3	0.1	160	1.0	48	—	—	—	—	—		~1	39.2	—
470					*Reduced temperature to 177°C and injected $H^{13}COOH$*													
470[d]	*0*	*61*	*0.06*	*230*	*0.66*	*<0.1*	*82*	*<0.1*	*25*	—	—				100	6	39.6	
639	169	75	21	204	0.78	<0.1	88	<0.1	29	—	—	—	—	—	100	6	33.8	4.6
1141	671	107	22	184	0.80	<0.1	100	<0.1	29	—	—	—	—	—	100	6	27.2	4.6
1171					*Increased temperature to 260°C and injected HCOOH*													
1171[d]	*0*	*59*	*12*	*257*	*0.44*	*<0.1*	*55*	*<0.1*	*16*	—	—	—	—	—	—	—	—	—
1262	91	327	219	3.8	0.48	<0.1	47	0.4	24	0.55	5.4	—	—	—	52	10	38.7	4.3
2104	933	323	234	4.0	0.81	<0.1	52	<0.1	23	0.70	9.0	—	0.6	<0.05	53	38	33.0	4.3
3257	2086	301	239	2.9	1.7	<0.1	74	<0.1	29	0.50	6.0	—	0.7	<0.05	55	61	28.3	4.4
3265					*Injected solution of NaOH and $MgCl_2$*													
3265[d]	*2094*	*168*	*133*	*1.6*	*0.96*	<0.1	*41*	<0.1	*16*	*0.30*	*3.3*	*108*	*179*	—	—	—	—	—
3306	2135	143	70	53	0.93	0.6	47	1.2	12	—	7.6	112	191	<0.05	53	61	43.8	7.3
4122	2951	118	57	50	0.97	<0.1	51	<0.1	31	0.42	7.0	112	179	<0.05	53	64	35.8	7.1
4217					*Temperature decreased to 175°C*													
4285	—	110	43	53	0.97	<0.1	52	<0.1	32	0.37	6.7	110	192	0.12	—	—	29.6	6.2
4307					*Injected solution of $H^{13}COOH$ and NaCl*													
4307[d]	*0*	*63*	*25*	*124*	*0.56*	*<0.1*	*30*	*<0.1*	*19*	*0.2*	*3.9*	*264*	*312*	*0.07*	—	—	—	—
4333	26	64	49	119	0.53	0.2	33	<0.1	23	<0.4	3.5	235	288	12	—	—	41.0	5.1
4983	676	102 (113)[e]	73 (80)[e]	69 (76)[e]	0.46	<0.1	39	<0.1	29	<0.4	4.0	213	251	17	—	—	35.2	4.9
4987					*Temperature raised to 225°C*													
4987[d]	*680*	*102*	*73*	*69*	*0.46*	*<0.1*	*39*	*<0.1*	*29*	*<0.4*	*2.9*	*213*	*251*	*17*	—	—	—	—
5030	723	102 (122)	77 (92)	40 (48)	0.43	<0.1	44	<0.1	35	<0.4	—	197	230	5.6	—	—	29.5	5.1
5341	1034	113 (147)	86 (112)	25 (32)	0.42	<0.1	52	<0.1	43	<0.4	4.1	181	213	0.4	78	56	24.3	5.6
5347					*Temperature lowered to 175°C*													
5418					*Injected $NaH^{13}CO3$ and NaOH in NaCl solution*													
5418[d]	*1111*	*55*	*92*	*12*	*0.20*	*<0.1*	*25*	*<0.1*	*21*		*2.0*	*272*	*360*	0.2	—	—	—	—
5437	1130	—	77	13	0.23	<0.1	30	<0.1	30	0.07	2.3	258	326	<0.05	—	—	37.3	7.0
6469	2162	39 (45)	50 (59)	27 (31)	0.22	<0.1	41	<0.1	37	0.07	2.1	221	266	<0.05	—	—	32.1	6.3

Concentrations are in mmol kg^{-1} (m) or μmol kg^{-1} (μ). "Dashes" = no data. The experiment initially contained 0.64 g powdered $NiFe_{1.4}$ and 39.2 g H_2O.

[a] Elapsed time since temperature increase to 260°C at 1171 h or injection of formic acid at 175°C at 4307 h.

[b] Estimated amount of fluid in reaction cell prior to sample.

[c] Calculated pH from fluid speciation (see "Methods").

[d] Concentrations shown in italics after each injection are calculated values based on the concentration prior to injection and the composition of the injected fluid.

[e] Values of H_2, ΣCO_2, and ΣFormate shown in parenthesis are recalculated to account for dilution of reaction cell contents (see text). The concentrations for time = t were calculated by multiplying the measured value by the ratio $[Cl]_{4333h \text{ or } 5437h}/[Cl]_t$.

in situ pH after injection of formic acid. The gold reaction cell apparently developed a small rupture during this injection, which is evident in the continuous gradual decrease in Cl concentration throughout the remainder of the experiment caused by diffusion of the cell contents into the surrounding pressurizing fluid (Cl-free H_2O) (Table 2). Since the rate of dilution of the cell contents by the pressurizing fluid appeared to be considerably slower than the rates of the reactions under study, it was decided that useful information could still be obtained and the experiment was continued. However, it should be understood that the measured concentrations of solutes in the remainder of the experiment are lowered by the dilution and, as a consequence, the apparent reaction rates are somewhat more rapid than the actual rates. The amount of dilution as indicated by the decrease in Cl concentration was used to gauge the loss of other solutes, and the concentrations of H_2, ΣCO_2, and ΣFormate corrected for loss by dilution are listed in parentheses in Table 2.

During the 676 h following the injection of $H^{13}COOH$ and NaCl at 4307 h, there was a decrease in the measured ΣFormate concentration and corresponding increases in ΣCO_2 and H_2 concentrations (Fig. 5a), indicating gradual decomposition of the injected ΣFormate. The rate of decomposition was comparable to that observed earlier in the experiment (Fig. 3a), indicating little or no effect of salinity on the decomposition reaction. Despite the gradual decomposition of ΣFormate, the experiment remained far from equilibrium after 676 h at 175°C (Fig. 5b).

At 4987 h, the temperature of the experiment was increased to 225°C. Within 33 h of the temperature increase, the measured ΣFormate concentration had decreased substantially, indicating an increase in the rate of decomposition with the increase in temperature (Fig. 5a; Table 2). The concentration of ΣFormate had decreased further by the time the second sample was obtained at this temperature 350 h later. However, by the time the second sample was taken, the measured $\Sigma CO_2/\Sigma$Formate ratio was very close to the calculated equilibrium value, suggesting that ΣCO_2 and ΣFormate had equilibrated well before this sample was taken (Fig. 5b). Extrapolation of the decomposition rate observed in the first 33 h suggests that equilibrium was attained within the first 75 h. The decomposition of ΣFormate was not accompanied by corresponding

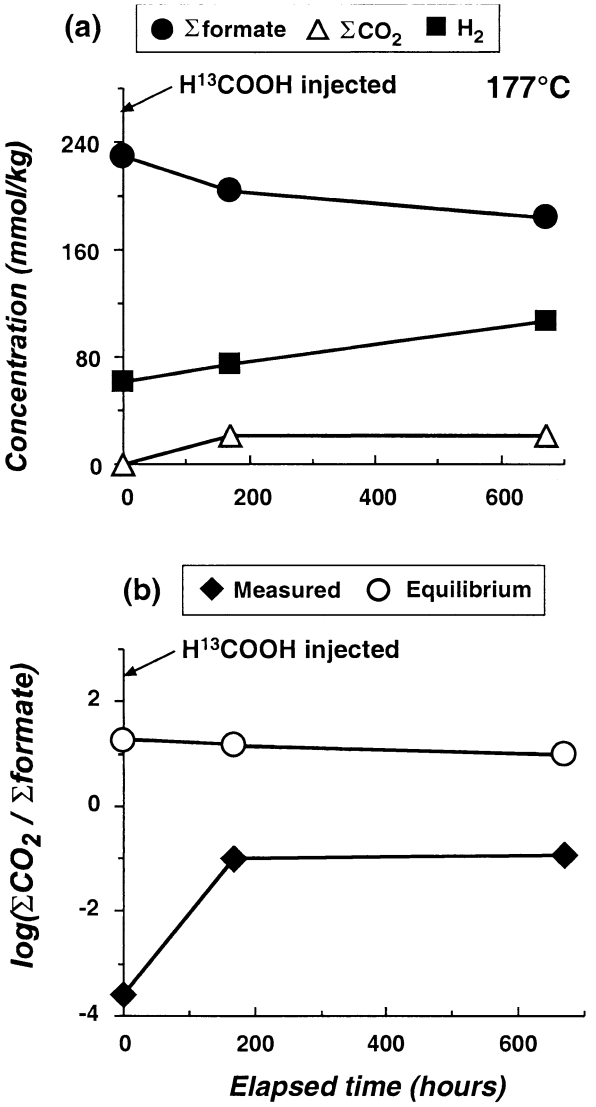

Fig. 3. (a) Measured concentrations of dissolved Σformate, ΣCO_2, and H_2 during reaction of aqueous solutions at 177°C in the NiFe alloy experiment as a function of elapsed time following injection of HCOOH at 470 h. (b) Comparison of calculated equilibrium ΣCO_2/Σformate ratios with the ratios measured in the experiment. Equilibrium ratios are calculated using the measured H_2 and estimated in situ pH for the corresponding sample.

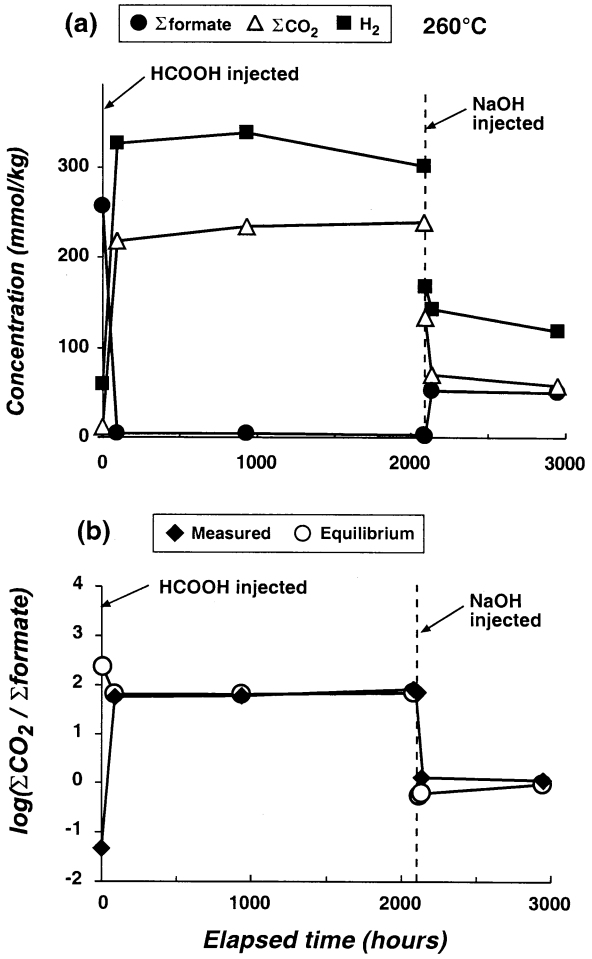

Fig. 4. (a) Measured concentrations of dissolved Σformate, ΣCO_2, and H_2 during reaction of aqueous solutions at 260°C in the NiFe alloy experiment as a function of elapsed time following injection of HCOOH at 1171 h. (b) Comparison of calculated equilibrium ΣCO_2/Σformate ratios with the ratios measured in the experiment. Equilibrium ratios are calculated using the measured H_2 and estimated in situ pH for the corresponding sample. The vertical line indicates injection of a NaOH solution at 2094 h elapsed time.

increases in the concentrations of ΣCO_2 and H_2. This observation, together with a decrease in the Mg concentration, indicates that much of the ΣCO_2 generated by Σformate decomposition was precipitated as Mg-Fe carbonates (Eqn. 7 and 9).

To observe the rate of ΣCO_2 reduction to formate at a lower temperature, the temperature of the experiment was again reduced to 175°C at 5347 h and a solution of $NaH^{13}CO_3$ plus NaOH injected at 5418 h. Gradual reduction of ΣCO_2 to formate was observed during ~1000 h of continued heating at this temperature, as indicated by an increase in Σformate concentration and corresponding decreases in H_2 and ΣCO_2 (Fig. 5a). However, the reaction still remained far from equilibrium when the experiment was terminated at 6469 h (Fig. 5b).

Solid products were collected by filtration at the termination of the experiment and analyzed by XRD and electron microprobe. The solids included magnetite, NiFe alloy, and carbonate minerals. Analysis of several NiFe alloy crystals by ion microprobe indicated they had a range of Fe contents from 2 to 9 mol.%. Carbonate minerals were primarily Mg-rich, with compositions ranging from $(Mg_{0.99}Fe_{0.01})CO_3$ to $(Mg_{0.92}Fe_{0.08})CO_3$, although a single carbonate grain with an anomalous composition of $(Mg_{0.23}Fe_{0.77})CO_3$ was observed.

3.1.1. *Production of methane and other hydrocarbons*

Methane and other hydrocarbons were observed in small amounts throughout the experiment (Table 2). Methane concentrations increased during the first 3300 h, and then remained essentially constant for the remainder of the experiment after taking into account dilutions during fluid injections (Fig. 6). In

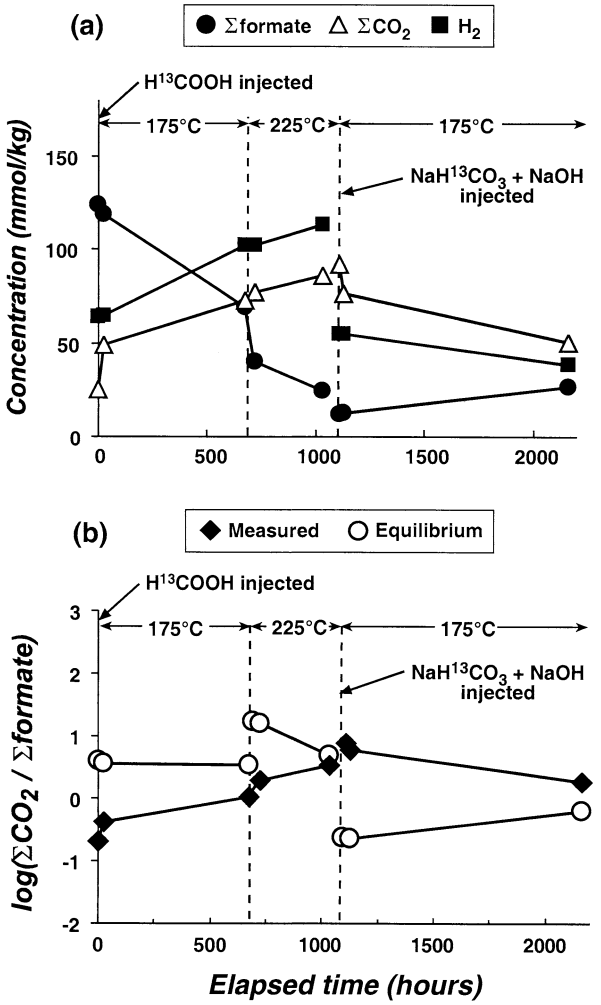

Fig. 5. (a) Measured concentrations of dissolved Σformate, ΣCO_2, and H_2 during reaction of aqueous solutions at 175 and 225°C in the NiFe alloy experiment as a function of elapsed time following injection of HCOOH at 4307 h. (b) Comparison of calculated equilibrium ΣCO_2/Σformate ratios with the ratios measured in the experiment. Equilibrium ratios are calculated using the measured H_2 and estimated in situ pH for the corresponding sample. The vertical lines indicate an increase in temperature to 225°C at 680 h elapsed time and a decrease in temperature to 175°C and injection of a $NaHCO_3$/NaOH solution at 1111 h.

general, the concentrations of other hydrocarbons such as ethane and propane increased only gradually throughout the experiment (Fig. 6). Hydrocarbons other than methane never accounted for more than a small fraction of the total dissolved carbon ($\ll$1%). Significant amounts of methanol were observed throughout this experiment (Table 2), but background levels of methanol were not determined so it is unclear whether the methanol resulted from reduction of CO_2.

Isotopic labeling was used to determine the amount of the methane and other hydrocarbons that were derived from injected carbon sources. Formic acid labeled with ^{13}C (99% $H^{13}COOH$) was injected at 470 and 4370 h, and the isotopic composition of ΣCO_2, methane, and C_2-C_6 hydrocarbons were monitored for samples taken between 639 and 4122 h and again at 5341 h (Table 2). The largest increase in methane concentration was observed between 1171 and 3257 h following an increase of the temperature to 260°C and injection of formic acid. A continuous increase in the proportion of ^{13}C in methane during this period (Table 2) indicates that the methane was mostly derived from the injected carbon source, which was present primarily as dissolved ΣCO_2 following rapid decomposition of formic acid after injection. At 3257 h, the proportion of ^{13}C in methane (61% $^{13}CH_4$) was essentially identical to the proportion in ΣCO_2 (55% $\Sigma^{13}CO_2$), demonstrating that the methane was derived from dissolved carbon and not from background sources. The proportions of ^{13}C in all hydrocarbons other than methane, however, remained at low levels ($\sim$1% ^{13}C) and were constant throughout the experiment, indicating that these hydrocarbons were generated from background sources rather than the injected carbon.

3.2. Reaction in the Presence of Serpentinized Olivine

This experiment was initiated by heating olivine with a 0.5 mol kg^{-1} NaCl solution at 330°C for 475 h, at which time the temperature was reduced to 177°C. During this period, strongly reducing conditions were generated within the reaction cell through the production of dissolved H_2 by the "serpentinization" reaction (Berndt et al., 1996; McCollom and Seewald, 2001):

$$\text{Olivine } (Fo_{88}) + 1.34\ H_2) \rightarrow 0.25 \text{ Serpentine} + 0.26 \text{ Brucite} + 0.08 \text{ Magnetite} + 0.08\ H_2. \quad (10)$$

Measurement of the fluid composition at 549 h (Table 3) showed that the H_2 concentration had increased to 55 mmol kg^{-1}. Small amounts of ΣCO_2, Σformate, and hydrocarbons were also observed at this time that were apparently derived from a background source associated with the minerals (Table 3).

A solution of ^{13}C-labeled bicarbonate (99% $NaH^{13}CO_3$) was injected into the experiment at 553 h to observe reduction of ΣCO_2 to formate. However, over the next 525 h at 177°C, the concentrations of all fluid components remained nearly constant (Fig. 7a). Based on thermodynamic considerations, a large fraction of the dissolved ΣCO_2 should have been reduced to formate under the reducing conditions present in the reaction vessel (Figs. 1a and 7b). Nevertheless, only a slight increase was observed in the measured Σformate concentration, indicating reduction of ΣCO_2 to formate was kinetically inhibited at the experimental conditions.

At 1079 h, a solution of $MgCl_2$ and $NaH^{13}CO_3$ was injected into the experiment to observe whether a decrease in pH would result in more rapid reduction of ΣCO_2. The injected $MgCl_2$ lowered pH through precipitation of brucite according to Eqn. 6. In addition to generating acidity, however, addition of $MgCl_2$ also had the unintended effect of removing almost all of the dissolved ΣCO_2 through precipitation of $MgCO_3$ (Eqn. 7) in addition to brucite. While the decrease in ΣCO_2 resulted in a measured ΣCO_2/Σformate ratio that was close to the expected equilibrium ratio for the conditions present in the reaction vessel (Fig. 7b), this can be attributed to mineral precipiation rather than reaction between ΣCO_2 and Σformate.

After this injection, there was essentially no change in the

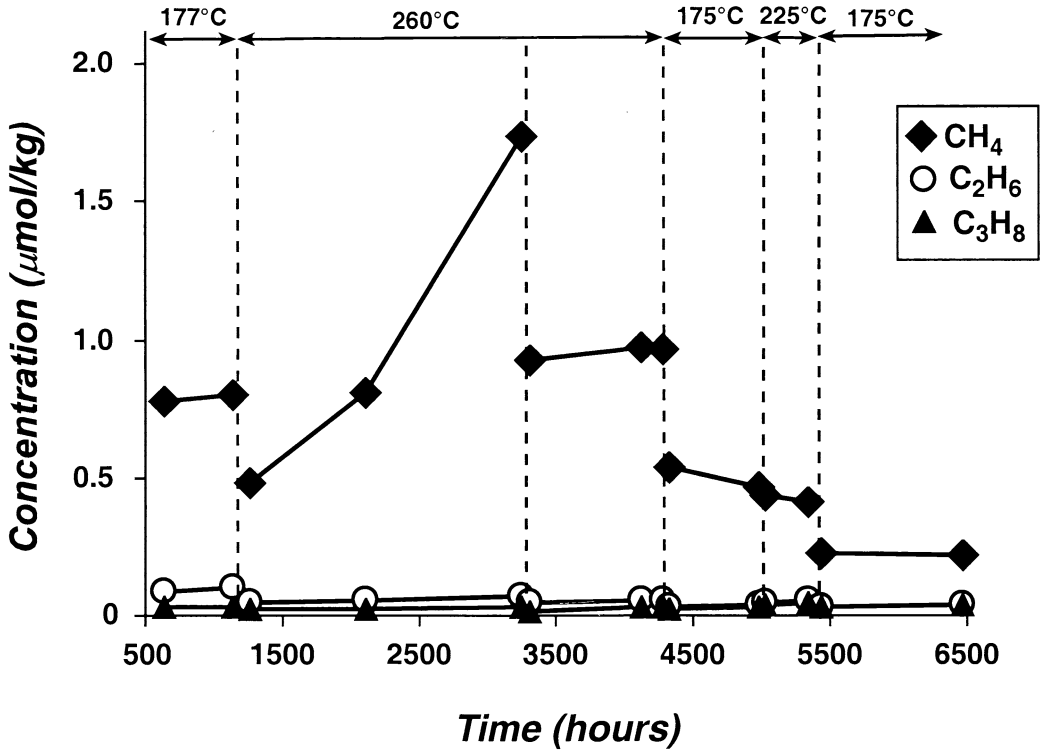

Fig. 6. Measured concentrations of dissolved methane, ethane, and propane during the NiFe alloy experiment. The vertical lines indicate changes in temperature or injection of reactant solutions.

concentrations of any solutes during 2300 h of additional heating at 177°C (Fig. 7a; Table 3). It was anticipated that this prolonged heating period might produce additional H_2 from serpentinization of olivine, which would subsequently result in an increase in formate concentration from ΣCO_2 reduction. However, no increase in H_2 concentration was observed during this period, suggesting that the serpentinization of olivine (Eqn. 10) was proceeding only very slowly, if at all, at this temperature.

The rate of formic acid decomposition was assessed at 177°C by injecting a solution of $H^{13}COOH$ at 3545 h. Partial dissociation of the injected $H^{13}COOH$ resulted in a slight decrease in pH, as reflected in an increase in Mg concentration from dissolution of magnesite and/or brucite (Table 3). The measured ΣCO_2 concentration also showed a slight increase immediately after the injection, but then decreased, apparently owing to reprecipitation of $MgCO_3$. During 680 h of additional heating at 177°C, only a small fraction of the injected formic acid decomposed, as indicated by a decrease of only 4 mmol kg^{-1} in the measured Σformate concentration and a corresponding increase in H_2 concentration (Fig. 7a). Thermodynamic calculations indicate that an equilibrium state would have required nearly complete decomposition of Σformate to H_2 and ΣCO_2 (Fig. 7b), indicating slow reaction kinetics for decomposition at this temperature.

Increasing the temperature to 250°C at 4225 h resulted in immediate and rapid decomposition of Σformate (Fig. 8a; Table 3). The nearly constant level of measured ΣCO_2 following the temperature increase, together with a decrease in Mg concentration, indicates that most of the ΣCO_2 produced by Σformate decomposition was precipitated as $MgCO_3$. Also, the increase in H_2 concentration observed during the 1482 h of heating following the temperature increase was greater than could be accounted for by decomposition of Σformate (Eqn. 1 and 3), suggesting that serpentinization of olivine had resumed with the increase in temperature. Comparison of the measured $\Sigma CO_2/\Sigma$formate ratio with that expected for equilibrium at the experimental conditions indicates that reactions between ΣCO_2 and Σformate equilibrated soon after the injection (Fig. 8b). The rapidity of the reaction suggests that equilibrium was probably attained well before the third sample was taken after 1482 h at this temperature, and probably was reached within ~600 h after the temperature increase.

In the final stage of this experiment, a solution of $NaH^{13}CO_3$ was injected at 5715 h to determine the rate of ΣCO_2 reduction to formate at 250°C (Table 3). A sharp increase in the measured Σformate concentration following the injection, along with corresponding decreases in H_2 and ΣCO_2 concentrations, indicated that much of the injected $NaH^{13}CO_3$ was rapidly reduced to formate (Fig. 8a). Attainment of steady state fluid composition in < 500 h after injection, combined with $\Sigma CO_2/\Sigma$formate ratios consistent with thermodynamic predictions (Fig. 8b) indicate rapid equilibration of ΣCO_2 and Σformate.

3.2.1. Production of methane and hydrocarbons

Trace amounts of dissolved methane as well as other hydrocarbons were observed during this experiment (Table 3). Once dilution during injections is accounted for, the levels of these compounds generally remained constant throughout the exper-

Table 3. Fluid composition during reaction of aqueous solutions with olivine.

Time (h)	ΔTime[a] (h)	H_2 (m)	ΣCO_2 (m)	ΣFormate (m)	CH_4 (μ)	C_2H_4 (μ)	C_2H_6 (μ)	C_3H_6 (μ)	C_3H_8 (μ)	ΣAcetate (m)	CH_3OH (m)	Cl (m)	Na (m)	Mg (m)	Ca (m)	Fluid[b] (g)	Calc. pH[c]
0							*Start of experiment; initial temperature = 330°C*										
139		18	—	0.14	—	—	—	—	—	0.32	—	—	—	—	—	31.7	
475							*Reduced temperature to 177°C*										
549	74	55	1.1	0.40	51	2.8	6.0	3.2	1.6	0.34	—	—	—	—	—	30.3	
553							*Injected solution of $NaH^{13}CO_3$*										
553[d]	*78*	*40*	*16*	*0.30*	*37*	*2.0*	*4.4*	*2.3*	*1.2*	*0.25*		*500*	*515*	—	—		
574	99	39	19	0.30	37	1.9	5.2	2.3	1.2	0.24	—	—	515	<0.05	<0.05	34.6	7.2
668	193	—	—	0.32	—	—	—	—	—	0.24	—	—	518	<0.05	<0.05	28.9	
1078	603	42	18	0.35	37	0.9	7.6	2.3	1.4	0.23	—	—	519	<0.05	<0.05	26.6	7.9
1079							*Injected $MgCl_2$ and $NaH^{13}CO_3$*										
1079[d]	*604*	*23*	*19*	*0.19*	*20*	0.5	*4.1*	1.2	*0.7*	*0.19*	—	*578*	*519*	*39*	*0*		
1150	675	22	0.3	0.19	20	0.3	3.6	1.1	0.7	0.12	—	—	517	23	1.8	40.2	6.3
1337	862	22	0.2	0.19	20	0.1	4.6	1.0	0.8	0.16	—	—	519	21	3.2	35.6	6.3
2495	2020	23	0.3	0.17	20	<0.1	4.5	0.7	1.2	0.11	—	—	528	20	3.2	32.4	6.2
3361	2886	22	0.2	0.20	21	<0.1	4.1	0.5	1.3	0.13	<0.04	—	517	21	4.3	27.1	6.3
3545							*Injected solution of $H^{13}COOH$*										
3545[d]	*3070*	*12*	*0.1*	*80*	*12*	*<0.1*	*2.2*	*0.3*	*0.7*	*0.07*	—	*532*	*498*	*12*	*2.4*		
3571	3096	12	3.2	80	11	<0.1	2.5	0.2	0.7	—	—	—	491	55	2.9	41.7	6.1
4222	3747	16	0.3	76	11	<0.1	2.2	0.2	0.9	—	—	—	489	50	2.5	36.8	6.1
4225							*Temperature increased to 250°C*										
4225[d]	*0*	*16*	*0.3*	*76*	*11*	*<0.1*	*2.2*	*0.2*	*0.9*	—	—	—	*489*	*50*	*2.5*	—	—
4269	44	36	4.3	47	11	<0.1	2.6	0.8	1.2	—	—	—	497	36	2.4	32.2	5.5
4581	356	88	1.4	3.2	12	<0.1	1.2	0.8	—	—	0.34	—	500	15	3.1	28.4	5.7
5707	1482	107	1.4	0.4	13	<0.1	1.8	0.8	1.3	0.12	—	—	508	8.3	3.3	23.9	5.8
5715							*Injected solution of $NaH^{13}CO_3$*										
5715[d]	*1490*	*62*	*56*	*0.2*	*6.7*	*<0.1*	*0.9*	*0.4*	*0.7*	*0.06*	—	*516*	*577*	*4.3*	*1.7*	—	—
5777	1552	46	40	13	7.8	<0.1	1.0	0.4	0.8	<0.1	0.13	—	593	<0.05	<0.05	38.0	8.9
6236	2011	41	29	26	8.8	<0.1	1.1	0.5	1.0	<0.1	0.13	—	601	<0.05	<0.05	32.2	8.2
6762	2537	46	27	29	10	<0.1	1.2	0.6	1.2	<0.1	0.14	—	577	<0.05	<0.05	26.6	8.4

Concentrations are in mmol kg^{-1} (m) or μmol kg^{-1} (μ). "Dashes" = no data. The experiment initially contained 20.7 g powdered olivine and 33.3 g 0.50 molal NaCl.

[a] Elapsed time since temperature reduction to 177°C at 475 h or increase to 250°C at 4225 h.

[b] Estimated amount of fluid in reaction cell prior to sample.

[c] Calculated pH from fluid speciation (see "Methods").

[d] Concentrations shown in italics after each injection or change in temperature are calculated values based on the concentration prior to injection and the composition of the injected fluid.

iment at the levels observed in the initial sample. The isotopic composition of the C_1-C_3 hydrocarbons were monitored by GCMS at 2495 and 6236 h. The hydrocarbons, including methane, had low proportions of ^{13}C (~1%) and showed no evidence of incorporation of the injected ^{13}C-labeled carbon sources ($NaH^{13}CO_3$ and $H^{13}COOH$). Consequently, there was no evidence for reduction of ΣCO_2 or Σformate to methane or other hydrocarbons in this experiment despite the strongly reducing conditions.

3.3. Reaction in the Presence of Hematite-Magnetite

A third experiment was conducted with the minerals hematite and magnetite included in the reaction cell. Hematite and magnetite are common minerals in sedimentary basins and hydrothermal environments, where they frequently exert a strong influence on the oxidation state of the fluid. In addition, these minerals have been found to be effective catalysts for the decomposition of acetic acid and acetate (Palmer and Drummond, 1986; Bell et al., 1994; McCollom and Seewald, 2003) and magnetite is reported to be an effective catalyst for synthesis of methane and complex hydrocarbons from reduction of CO_2 (e.g., Satterfield et al., 1986; Chen and Bahnemann, 2000).

The experiment was initiated by heating the minerals with pure water for 146 h at 250°C. At 141 h, analysis of the fluid indicated an H_2 concentration of 0.008 mmol kg^{-1} and trace amounts of ΣCO_2, Σformate, and hydrocarbons (Table 4). At 146 h, a solution of ^{13}C-labeled formic acid (99% $H^{13}COOH$) was injected into the experiment. Within 140 h after the injection, most of the formic acid had decomposed to ΣCO_2 and H_2 (Fig. 9a; Table 4). The measured concentration of H_2 was less than would be expected for the amount of formic acid decomposed, indicating that some of the H_2 was consumed by reduction of hematite to magnetite. The measured ΣCO_2/Σformate ratio 140 h after the injection was close to the ratio expected for equilibrium at 250°C for the measured H_2 concentration and estimated pH (Fig. 9b), suggesting that ΣCO_2 and Σformate had attained equilibrium by this time.

Only small increases were observed in the concentrations of methane and other hydrocarbons after the injection. While dissolved ΣCO_2 and Σformate were predominantly ^{13}C labeled (>98% ^{13}C) in a fluid sample at 286 h, all C_1-C_3 hydrocarbons had low proportions of ^{13}C (~1%). Larger hydrocarbons were below detection limits. Consequently, there was no evidence for formation of hydrocarbons from reduction of ΣCO_2 or Σformate in this experiment.

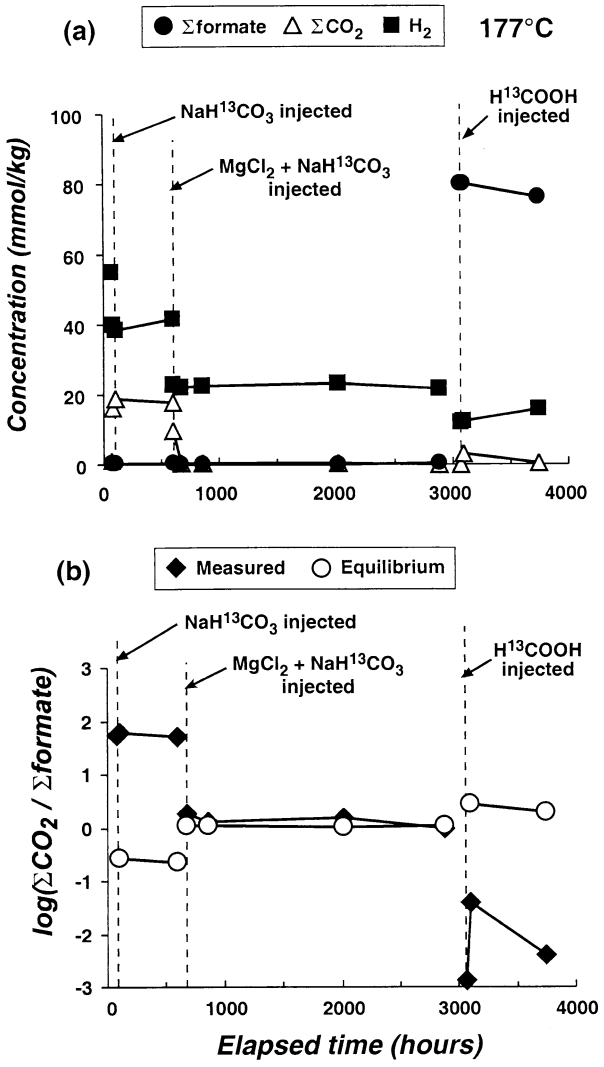

Fig. 7. (a) Measured concentrations of dissolved Σformate, ΣCO_2, and H_2 during reaction of aqueous solutions at 177°C in the olivine experiment as a function of elapsed time after temperature reduction at 475 h. (b) Comparison of calculated equilibrium $\Sigma CO_2/\Sigma$formate ratios with the ratios measured in the experiment. Equilibrium ratios are calculated using the measured H_2 and estimated in situ pH for the corresponding sample. The vertical lines indicate injection of reactant solutions at 78, 604, and 3070 h elapsed time.

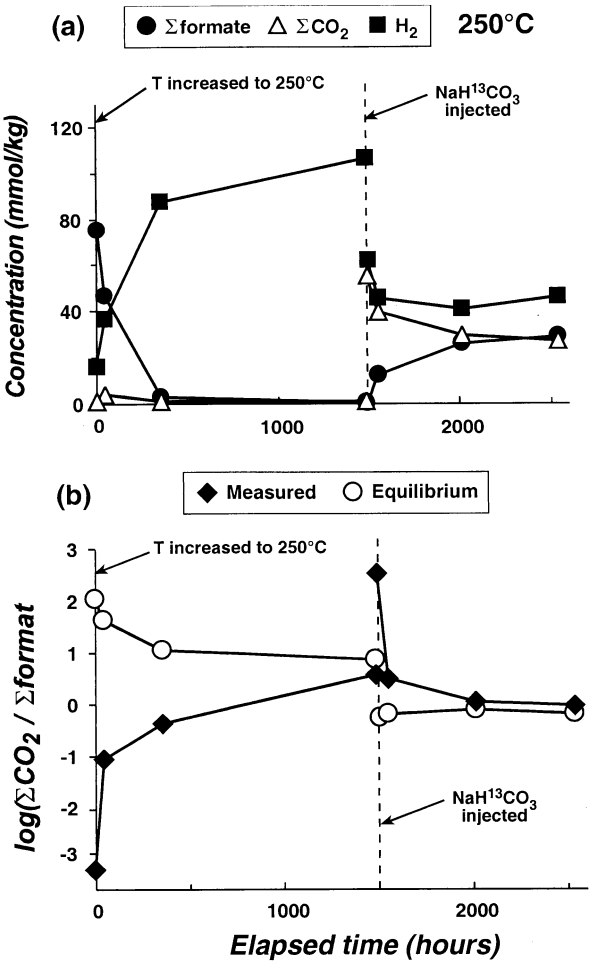

Fig. 8. (a) Measured concentrations of dissolved Σformate, ΣCO_2, and H_2 during reaction of aqueous solutions at 250°C in the olivine experiment as a function of elapsed time following injection of HCOOH at 4225 h. (b) Comparison of calculated equilibrium $\Sigma CO_2/\Sigma$formate ratios with the ratios measured in the experiment as a function of reaction time. Equilibrium ratios are calculated using the measured H_2 and estimated in situ pH for the corresponding sample. The vertical line indicates injection of a $NaHCO_3$ solution at 1490 h elapsed time.

3.4. Reaction in the Absence of Minerals ("Mineral-Free" Experiment)

For comparison with the previous results, an additional formic acid experiment was conducted in the gold-titanium reaction cell with no minerals present. This experiment was intended to provide a baseline to evaluate the extent to which the presence of minerals enhanced the rate of decomposition. For this experiment, a solution of formic acid was injected into a mineral-free reaction cell containing water and minor amounts of H_2 and ΣCO_2 at 250°C (Table 5). Most of the injected formic acid had decomposed to ΣCO_2 and H_2 within 69 h of the injection (Fig. 10a). The measured $\Sigma CO_2/\Sigma$formate ratio after 69 h was close to the ratio expected for equilibrium at 250°C for the measured H_2 concentration and estimated in situ pH of ~4.1 (Fig. 10b), suggesting that ΣCO_2 and Σformate had attained equilibrium by this time.

4. DISCUSSION

4.1. Decomposition of Formic Acid and Formate

The measurements of Σformate decomposition from this study are summarized in Figure 11. Rapid decomposition of injected Σformate was observed in each of the experiments conducted at temperatures of 225°C or higher (Fig. 11b). Gradual decomposition was also observed in the NiFe experiment at 175 and 177°C (Fig. 11a). Conversely, while there was a slight decrease in the measured Σformate concentration following injection of formic acid into the olivine experiment at 177°C (3545–4222 h), the decrease was within the analytical error of

Table 4. Fluid composition during reaction of a formic acid solution with hematite-magnetite at 250°C, 350 bars.

Time (h)	ΔTime[a] (h)	H_2 (m)	ΣCO_2 (m)	ΣFormate (m)	CH_4 (μ)	C_2H_4 (μ)	C_2H_6 (μ)	C_3H_6 (μ)	C_3H_8 (μ)	CH_3OH (m)	Fluid[b] (g)	Calc. pH[c]
0				*Start of experiment; initial temperature = 250°C*								
141		0.008	0.96	0.016	1.7	0.2	0.06	0.2	0.02	—	36.1	—
146				*Injected solution of $H^{13}COOH$*								
146[d]	*0*	*.006*	*0.7*	*190*	*1.3*	*0.1*	*0.04*	*0.1*	*0.01*	—	—	—
160	14	—	—	106	—	—	—	—	—	—	36.3	—
171	25	88	123	69	1.9	0.2	0.07	1.0	0.04	—	34.2	4.0
192	46	113	166	36	2.4	0.2	0.08	—	—	—	29.9	4.1
286	140	126	204	3.9	3.5	0.2	0.16	1.2	0.13	0.34	26.1	4.4

Concentrations are in mmol kg^{-1} (m) or μmol kg^{-1} (μ). "Dashes" = no data. The experiment initially contained 8.1 g Fe_2O_3, 0.64 g Fe_3O_4 and 36.1 g H_2O.

[a] Elapsed time since injection of formic acid solution at 146 h.

[b] Estimated amount of fluid in reaction cell prior to sample.

[c] Calculated pH from fluid speciation (see "Methods").

[d] Concentrations shown in italics after each injection or change in temperature are calculated values based on the concentration prior to injection and the composition of the injected fluid.

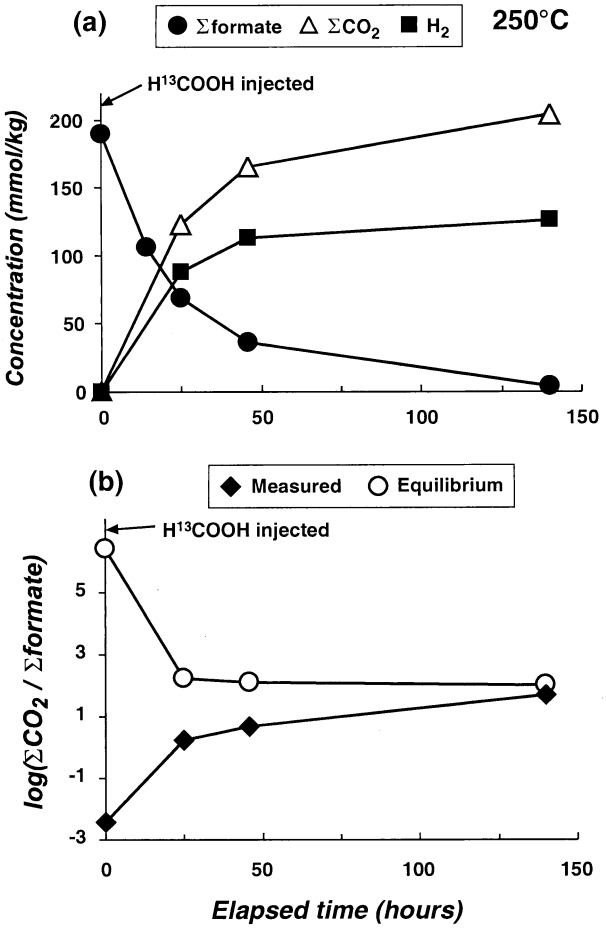

Fig. 9. (a) Measured concentrations of dissolved Σformate, ΣCO_2, and H_2 during reaction of aqueous solutions at 250°C in the hematite-magnetite experiment. (b) Comparison of calculated equilibrium ΣCO_2/Σformate ratios with the ratios measured in the experiment as a function of reaction time. Equilibrium ratios are calculated using the measured H_2 and estimated in situ pH for the corresponding sample.

the measurements. Consequently, it appears that little or no decomposition of Σformate occurred in the presence of serpentinized olivine during > 700 h of heating at 177°C.

In previous studies, decomposition of aqueous formic acid has been found to follow reaction kinetics that are first-order with respect to the formic acid concentration (Bjerre and Sørensen, 1992; Maiella and Brill, 1998; Yu and Savage, 1998). In our experiments, decomposition of Σformate generally followed linear trends on plots of log [Σformate] vs. reaction time (Fig. 11), which would be consistent with first-order reaction kinetics. To facilitate comparison with previous results, we fit our decomposition results with a first-order kinetic rate law of the form

$$d\left[\sum \text{formate}\right]/dt = k_{\text{decomp}}\left[\sum \text{formate}\right] \qquad (11)$$

where k_{decomp} is the rate constant for the overall decomposition of Σformate and t the elapsed time. It must be noted, however, that many of our experiments contained too few data points to unambiguously determine reaction parameters, particularly in

Table 5. Fluid composition during reaction of a formic acid solution in the absence of minerals at 250°C, 350 bars.

Time (h)	ΔTime[a] (h)	H_2 (m)	ΣCO_2 (m)	ΣFormate (m)
0		*Start of experiment*		
0		9	11	6
2		*Injected $H^{13}COOH$ sol'n.*		
2[b]	*0*	*4*	*4.6*	*178*
9.5	7.5	—	—	55
12.5	10.5	—	—	41
23.5	21.5	174	151	30
71	69	193	170	5.1

Concentrations are in mmol kg^{-1} (m).

[a] Elapsed time since injection of formic acid solution at 2 h.

[b] Concentrations shown in italics after each injection are calculated values based on the concentration prior to injection and the composition of the injected fluid.

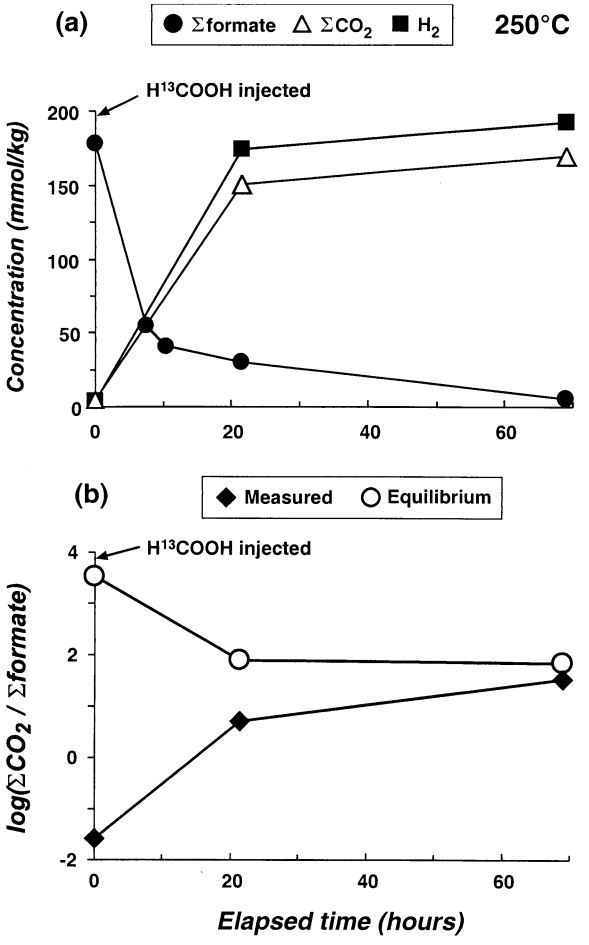

Fig. 10. (a) Measured concentrations of dissolved Σformate, ΣCO_2, and H_2 during reaction of aqueous solutions at 250°C in the mineral-free experiment. (b) Comparison of calculated equilibrium ΣCO_2/Σformate ratios with the ratios measured in the experiment as a function of reaction time. Equilibrium ratios are calculated using the measured H_2 and calculated pH for the corresponding sample.

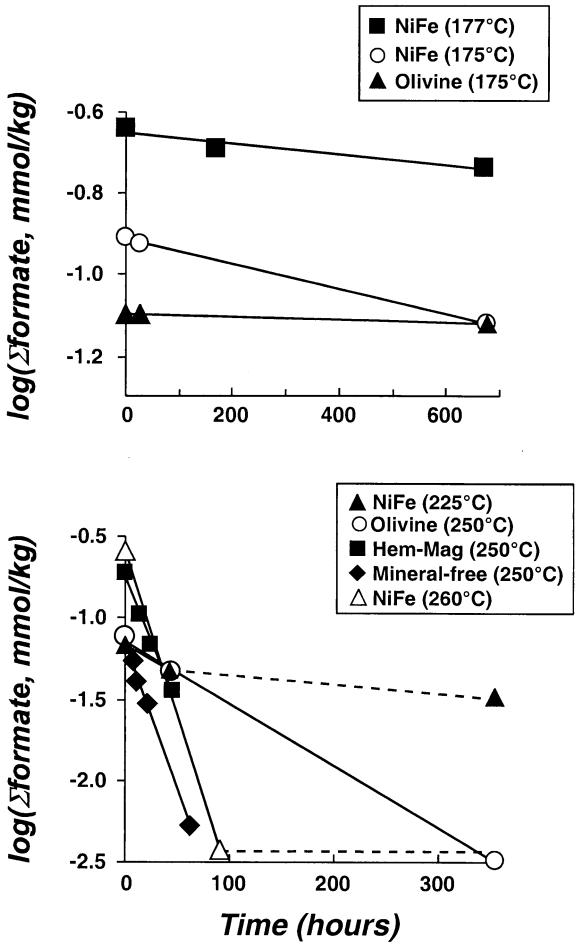

Fig. 11. Measured concentrations of Σformate in the hydrothermal experiments as a function of elapsed time following injection of formic acid or increase in reaction temperature. The solid lines represent linear regression fits to the data. Dashed lines indicate intervals where Σformate had apparently equilibrated with dissolved ΣCO_2. Data in these intervals are not included in regressions to determine rate constants (see text).

the case of experiments that equilibrated with ΣCO_2 before the second or third measurement. Because of these limitations, the evaluation of reaction kinetics presented here should be considered as preliminary rather than definitive.

Values of k_{decomp} determined from linear regression of the data shown in Figure 11 are summarized in Table 6 and plotted in Figure 12a. Determination of these values of k_{decomp} required a number of approximations to be made. Although the olivine and hematite-magnetite results at 250°C could be accurately fit with Eqn. 11, the mineral-free decomposition experiment at 250°C exhibited a poor fit to first-order reaction kinetics ($R^2 = 0.937$). This poor fit appears to be attributable to decomposition that was faster than expected during the period immediately following the formic acid injection. Formic acid was injected into the experiment as a highly concentrated solution, and decomposition of formic acid within this concentrated fluid before complete mixing with the other ingredients in the reaction cell would have been more rapid than for the bulk fluid. Therefore, the calculated concentration of Σformate following injection was eliminated from the regression, and values of k_{decomp} for the mineral-free experiment given in Table 6 and Figure 12 represent a fit to the measured Σformate concentrations for the period 7.5 to 69 h after injection. This modified regression exhibits a good fit to first-order kinetics ($R^2 = 0.995$). For the NiFe experiment at 225°C, Σformate had apparently reached thermodynamic equilibrium with ΣCO_2 before the second sample was taken at 1034 h (Fig. 5), so only the initial concentration and first sample were used to estimate the rate constant for this stage. Also, for the NiFe experiment at 260°C, thermodynamic equilibrium was apparently attained before the first sample was taken 91 h after the injection of formic acid. Consequently, the rate constant for this stage of the experiment represents a minimum value. The rate constant given in Table 6 for the olivine experiment at 177°C represents the maximum rate consistent with the lack of measurable Σformate decomposition for that stage of the experiment.

Included in Figure 12, for comparison, are first-order rate constants from previous studies of aqueous formic acid and formate decomposition (Crossey, 1991; Bjerre and Sørensen,

Table 6. Rate constant data for decomposition of formic acid.

Experiment	Temp. (°C)	k_{decomp} (s^{-1})	In situ pH[a]	F_{HCOOH}[b]	k_{HCOOH} (s^{-1})	k_{HCOO^-} (s^{-1})
NiFe (470–671 h)	177	8.4×10^{-8}	4.6	0.16	3.0×10^{-7}	4.4×10^{-8}
NiFe (4307–4903 h)	175	2.0×10^{-7}	5.1	0.09	8.7×10^{-7}	1.3×10^{-7}
NiFe (4987–5341 h)	225	2.4×10^{-6}	5.1	0.18	7.7×10^{-5}	1.2×10^{-6}
NiFe (1171–3257 h)[c]	260	$>1.3 \times 10^{-5}$	4.3	0.76	$>1.6 \times 10^{-5}$	$>2.3 \times 10^{-6}$
Olivine (3545–4222 h)[d]	175	$<2.1 \times 10^{-8}$	6.1	0.01	$<1.4 \times 10^{-7}$	$<2.0 \times 10^{-8}$
Olivine (4225–5707 h)	250	2.4×10^{-6}	5.5	0.10	1.0×10^{-5}	1.6×10^{-6}
Hematite-magnetite	250	1.0×10^{-5}	4.0	0.80	1.2×10^{-5}	1.8×10^{-6}
Mineral-free	250	1.0×10^{-5}	3.1	0.98	1.0×10^{-5}	—

[a] In situ pH estimated from fluid speciation calculations.
[b] Estimated fraction of Σformate present as formic acid (HCOOH).
[c] The rate constants shown for the NiFe experiment at 260°C are minimum values since thermodynamic equilibrium between ΣCO_2 and Σformate had was apparently reached before the first sample was obtained.
[d] Values for the olivine experiment at 175°C correspond to the maximum reaction rate that would be consistent with the lack of detectable decomposition in the experiments.

1992; Small and Manning, 1993; Maiella and Brill, 1998; Yu and Savage, 1998; McCollom and Seewald, 2001). Yu and Savage (1998) conducted experiments for a range of water densities from liquid to vapor, and only those results for liquid-like fluid densities are shown in Figure 12. Also, the data for Yu and Savage (1998) shown in Figure 12 differ from those given by the original authors because the values shown in the figure were determined from linear regression of plots of log [HCOOH] vs. reaction time similar to Figure 11, whereas the values given in the original paper were determined from linear fits of log {1/(1 − [HCOOH])} vs. reaction time. The values for Crossey (1991) shown in Figure 12 are derived from regression of log [Σformate] vs. reaction time for decomposition in mixed acetate/formate solutions at pH 4 and 7. The rate constant for Small and Manning (1993) is determined from a linear regression of their reported concentrations of formate. In their experiments, which were conducted in a gold-titanium reactor similar to that employed in this study, formate was generated from decomposition of potassium oxalate, which they used as a source of K in a study of illite precipitation. The rate constant shown for McCollom and Seewald (2001) represents a minimum value since Σformate and ΣCO_2 had apparently reached thermodynamic equilibrium by the time their first sample was obtained.

The data in Figures 11 and 12a show that the rate of decomposition of Σformate in the olivine experiment at 177°C was significantly slower than in the NiFe experiment at similar temperatures. Reaction of Σformate at 250°C in the olivine experiment also proceeded much more slowly than in the hematite-magnetite and mineral-free experiments at this temperature. At 250°C, decomposition in the olivine experiment was only as fast as decomposition in the NiFe experiment at 225°C.

It appears unlikely that mineral catalysis can account for these differences in reaction rates since the rates were actually slower in the olivine and hematite-magnetite experiments at 250°C than in the mineral-free experiment at the same temperature. The most reasonable explanation for these differences in reaction rates appears to involve the pH of the reactant aqueous solutions and the speciation of Σformate. Although Σformate was injected into the experiments in the form of formic acid ($HCOOH_{(aq)}$), interaction with preexisting fluid and minerals in the reaction cell would have caused some of the injected acid to be converted to formate ($HCOO^-$) and metal-formate complexes with Fe, Mg, Na, or Ca (Me-HCOO). Higher pH in the olivine experiment would have favored the conversion of a higher percentage of the injected formic acid into formate. Previously, Maiella and Brill (1998) observed that decarboxylation of sodium formate solutions proceeded at a rate that was 41 to 65% slower than decarboxylation of formic acid solutions under the same conditions (Fig. 12a). Consequently, high pH solutions in which a higher proportion of the total formate was present as $HCOO^-$ would be expected to exhibit a slower rate of overall Σformate decomposition.

Considering the potential effect of speciation on reaction rates, first-order kinetics for Σformate decomposition would be more completely expressed by the relationship

$$d\left[\sum \text{formate}\right]/dt = k_{HCOOH}[HCOOH_{(aq)}] + k_{HCOO^-}[HCOO^-] + k_{\text{Me-HCOO}}\,[\text{Me-HCOO}] \quad (12)$$

where k_{HCOOH}, k_{HCOO^-}, and $k_{\text{Me-HCOO}}$ are rate constants for decomposition of formic acid, formate, and metal-formate complexes, respectively. Our experimental data do not allow values of k_{HCOOH}, k_{HCOO^-}, and $k_{\text{Me-HCOO}}$ to be determined independently. However, if we make the simplifying assumptions that metal-formate complexes decompose at approximately the same rate as formate ($k_{HCOO^-} \approx k_{\text{Me-HCOO}}$), Eqn. 12 can be reduced to

$$d\left[\sum \text{formate}\right]/dt = \{k_{HCOOH}F_{HCOOH} + k_{HCOO^-}(1 - F_{HCOOH})\}\left[\sum \text{formate}\right] \quad (13)$$

where F_{HCOOH} is the proportion of $HCOOH_{(aq)}$ in Σformate. This relationship can be equated with Eqn. 11 to yield

$$k_{decomp} = [k_{HCOOH}F_{HCOOH} + k_{HCOO^-}(1 - F_{HCOOH})]. \quad (14)$$

Values of F_{HCOOH} for the experiments can be calculated from the estimated in situ pH together with dissociation constants for formic acid at the experimental conditions deter-

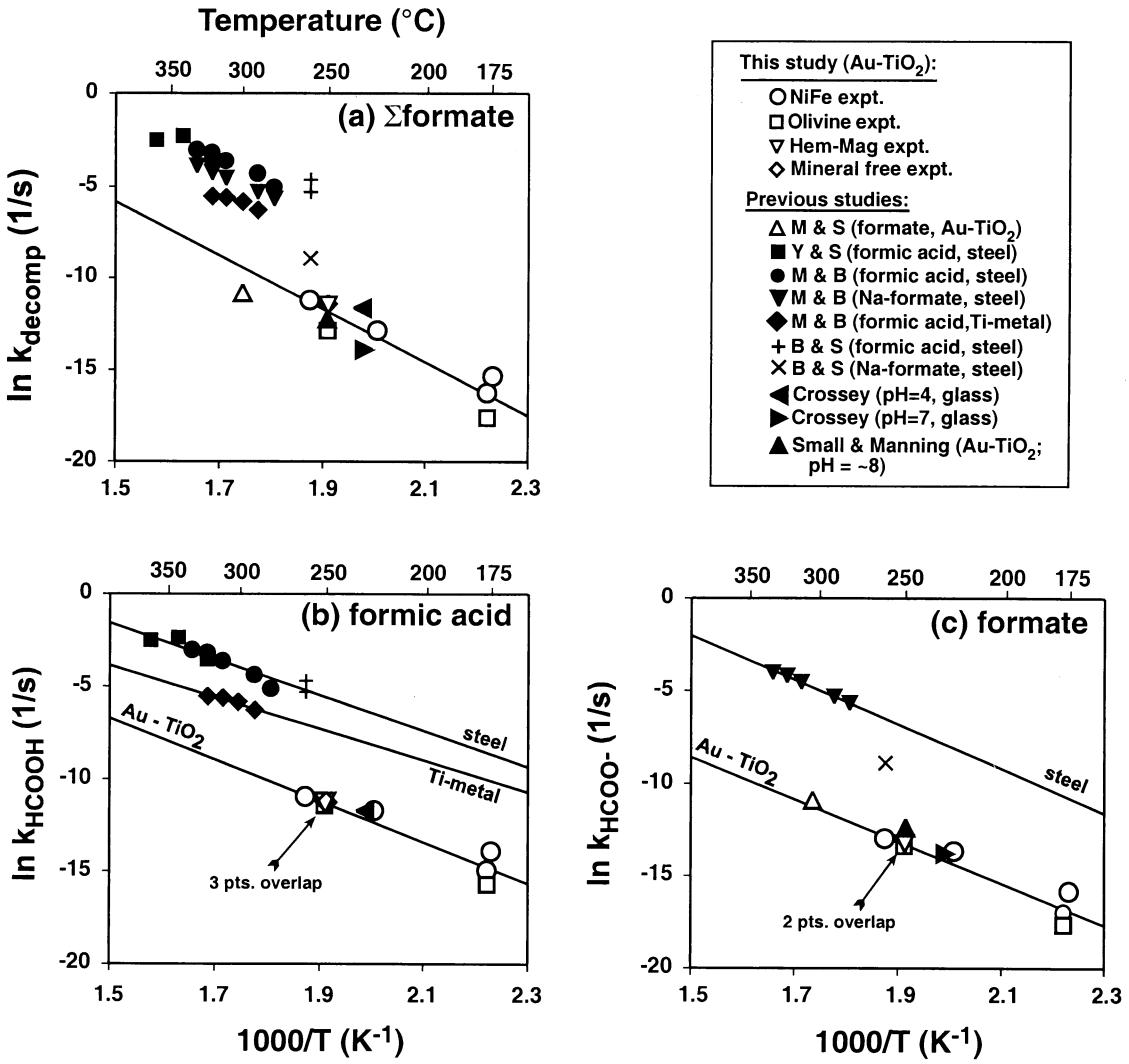

Fig. 12. First-order rate constants for Σformate decomposition as a function of temperature expressed as 1000/*T*. (a) Overall rate constant, k_{decomp}, for decomposition of total formate (Σformate). (b) Rate constants for formic acid decomposition (k_{HCOOH}). (c) Rate constants for formate decomposition (k_{HCOO^-}). Lines represent linear regressions of the data (see text). Also shown in the plots are data from Crossey (1991), Bjerre and Sørensen (1992) (B & S), Maiella and Brill (1998) (M & B), Yu and Savage (1998) (Y & S), Small and Manning (1993) (S & M), and McCollom and Seewald (2001) (M & S).

mined using thermodynamic parameters given by Shock (1995). Calculated values of F_{HCOOH} for the experiments are given in Table 6. In the mineral-free experiment, the injected formic acid apparently would have undergone little dissociation (calculated $F_{HCOOH} = 0.98$) suggesting that the Σformate decomposition rate measured for this experiment is almost entirely attributable to decomposition of formic acid. The data for this experiment yield a rate constant for formic acid decomposition (k_{HCOOH}) at 250°C equal to 1.0×10^{-5} s^{-1}. If we assume that this value reflects formic acid decomposition during the olivine experiment at 250°C, a value of 1.6×10^{-6} s^{-1} is retrieved for k_{HCOO^-} using Eqn. 14. Comparison of these rates constants suggests that formate decomposed at a rate that was ~85% slower than formic acid. Assuming that the relative rates of decomposition for formic acid and formate were similar in all experiments (i.e., $k_{HCOO^-} = 0.15 \times k_{HCOOH}$), Eqn. 14 can be used to calculate values of k_{HCOOH} and k_{HCOO^-} for the other experiments. Resulting values for the rate constants are listed in Table 6 and plotted in Figures 12b and 12c. This approach, which takes into account the effects of pH on reaction rates, results in a considerable reduction in the scatter in rate constants among experiments.

The similarity of reaction rates for experiments at the same or similar temperatures in this study as shown in Figures 12b and 12c indicates that minerals surfaces did not promote the decomposition of formic acid or formate, although they did have an indirect effect on reaction rates through their influence on pH-dependent Σformate speciation. The reaction rates measured in this study are also consistent with those measured in glass reaction vessels by Crossey (1991) and in a gold-TiO_2 vessel by Small and Manning (1993). On the other hand, the rates measured in this study were much slower than those

Table 7. Arrhenius parameters for decomposition of formic acid and formate.

Reaction	A (s^{-1})	E_a (kJ mol^{-1})
Σformate decomposition (k_{decomp})	8.1×10^6	120.9
Formic acid decomposition (k_{HCOOH})		
Au-TiO_2 (this study)	2.7×10^4	93.6
Steel	4.5×10^5	81.0
Ti-metal	7.4×10^3	70.9
Formate decomposition (k_{HCOO^-})		
Au-TiO_2 (this study)	5.2×10^3	94.6
Steel	8.9×10^6	99.8

measured in previous studies conducted in steel and Ti-metal reaction vessels, indicating that reaction rates in those studies were accelerated by interaction with the vessel walls.

The Arrhenius equation relates reaction rate constants as a function of temperature to the activation energy according to

$$\ln k = \ln A - E_a/(RT) \quad (15)$$

where A is a preexponential factor, E_a is the activation energy, R is the universal gas constant, and T is the temperature (K). Values of A and E_a for decomposition of formic acid and formate determined from linear fits of the rate constants shown in Figure 12 are listed in Table 7. For the regressions, the previous experiments conducted in steel and Ti-metal reactors are considered separately from the experiments in this study, and are assumed to represent steel- and Ti-catalyzed decomposition of formic acid and formate. The regression for Au-TiO_2 included all data for experiments in the present study, but did not include data from McCollom and Seewald (2001), Crossey (1991), and Small and Manning (1993) that appear to be consistent with this trend.

4.2. Reduction of Dissolved CO_2 to Formate

Reduction of ΣCO_2 to formate was observed in the olivine experiment at 250°C and in the NiFe experiment at 175 and 260°C following either the injection of $NaHCO_3$ or the injection of NaOH to increase pH (Figs. 4, 5, and 7). The reaction proceeded rapidly at the higher temperatures, so that equilibrium between ΣCO_2 and Σformate was attained within a short time after the injection (<200 h). McCollom and Seewald (2001) also observed rapid reduction of ΣCO_2 to formate in the presence of serpentinized olivine at 300°C, with equilibrium attained in < 24 h. Although reduction of dissolved ΣCO_2 to formate was observed in the NiFe experiment at 175°C, no measurable reduction was observed after injection of $NaHCO_3$ into the olivine experiment at 177°C over a similar time interval (Fig. 7). Since these experiments were apparently at similar pH, the results suggest that mineral surfaces in the NiFe experiment may have catalyzed the reduction reaction to some degree.

The available data are not sufficient to allow a rigorous analysis of reaction rates for ΣCO_2 reduction. However, since preliminary kinetic data may nevertheless be useful for geochemical modeling and for designing future experiments, we constructed a simple kinetic model for our experimental data (Fig. 13). In this model, we assumed that ΣCO_2 reduction was

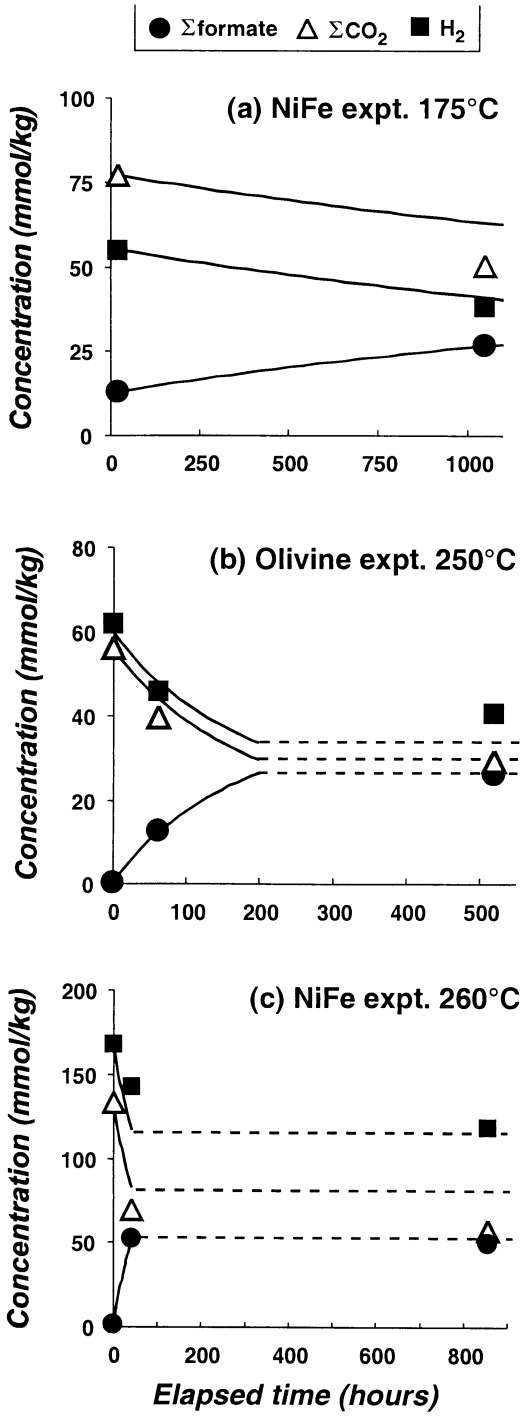

Fig. 13. Kinetic model fits for ΣCO_2 reduction. The symbols represent the measured concentrations of Σformate, ΣCO_2, and H_2 during hydrothermal experiments, and the solid lines represent results of kinetic model fits to these data (see text). The dashed lines indicate intervals where Σformate and ΣCO_2 had apparently attained thermodynamic equilibrium.

first order with respect to the concentrations of both ΣCO_2 and H_2. Accordingly, the increase in Σformate abundance from ΣCO_2 reduction could be portrayed by the relationship

Table 8. Rate constant data for reduction of ΣCO_2 to Σformate.

Experiment	Temp. (°C)	k_{red} ($mmol^{-1}$ s^{-1})
NiFe	175	1.1×10^{-9}
NiFe	260	1.9×10^{-8}
Olivine[a]	177	$<6.9 \times 10^{-11}$
Olivine	250	1.9×10^{-8}
M & S[b]	300	$>8.9 \times 10^{-8}$

[a] The rate constant for olivine at 177°C is the maximum rate that would be consistent with the lack of detectable reduction.

[b] Rate constant calculated from data in McCollom and Seewald (2001). The value shown is a minimum since thermodynamic equilibrium between ΣCO_2 and Σformate had apparently been reached before the first sample was obtained.

$$d\left[\sum \text{formate}\right]/dt = k_{red}\left[\sum CO_2\right][H_2] \quad (16)$$

where k_{red} is the rate constant for reduction of dissolved ΣCO_2 to formate. Since the reaction may involve either $CO_{2(aq)}$ or HCO_3^-, or both, k_{red} is an effective overall rate constant that may represent more than one concurrent reaction. Corresponding decreases in ΣCO_2 and H_2 are portrayed by

$$d\left[\sum CO_2\right]/dt = d[H_2]/dt = -d\left[\sum \text{formate}\right]/dt. \quad (17)$$

The initial concentrations of ΣCO_2, Σformate, and H_2 following injection of $NaHCO_3$ or NaOH were used as the starting point for the models (Tables 2 and 3), and values of k_{red} were adjusted to fit the calculated concentrations to those measured in the experiments as a function of reaction time. Since the concentrations of both ΣCO_2 and H_2 can be affected by reactions with minerals, the models were optimized to fit the measured Σformate concentrations. In addition, because the higher temperature experiments apparently attained equilibrium soon after the $NaHCO_3$ injection, the rate model was discontinued once the apparent equilibrium concentration of Σformate was reached. For the 260°C NiFe experiment results, the experiment had already reached equilibrium by the time the first sample was taken 41 h after the injection of NaOH at 3265 h. Consequently, the rate determined from the model for this experiment is a minimum value.

The results of the kinetic models are shown in Figure 13, and the values of k_{red} determined from the best fits of the models to the experimental data are given in Table 8. Values of k_{red} are plotted in Figure 14 as a function of experiment temperature expressed as 1000/*T*. Also shown in Figure 14 is the maximum value of k_{red} that would be consistent with the lack of any measurable ΣCO_2 reduction in the olivine experiment at 175°C, as well as a minimum value of k_{red} for the reduction of ΣCO_2 to Σformate from the data of McCollom and Seewald (2001). Regression of the rate constants shown in Figure 14 yield Arrhenius parameters of $A = 0.26\ mmol^{-1}\ kg^{-1}\ s^{-1}$ and $E_a = 71.7\ kJ\ mol^{-1}$.

For illustrative purposes, these parameters were used to calculate half-lives ($t_{1/2}$) of ΣCO_2 for a range of temperatures. The half-lives were calculated for both strongly reducing conditions (H_2 assumed to be constant at 50 mmolal) and mildly

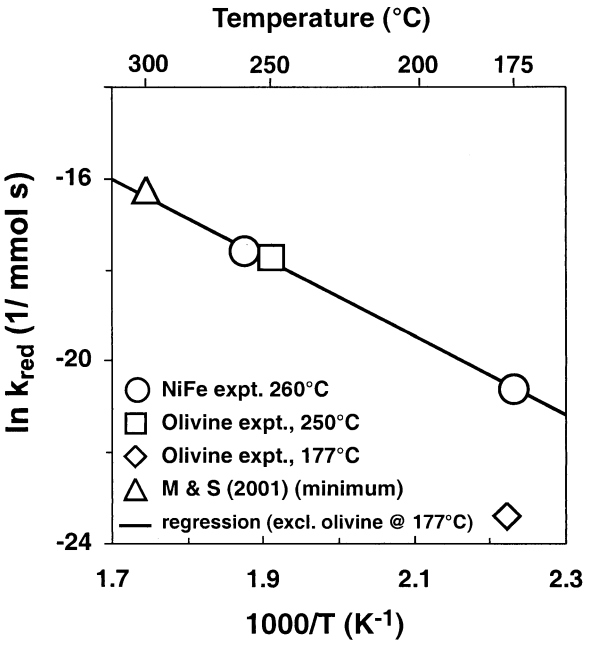

Fig. 14. Rate constants for ΣCO_2 reduction determined from the rate models shown in Figure 12, plotted as a function of temperature expressed as 1000/*T*. The line represents a regression to the data, excluding the olivine experiment at 177°C.

reducing conditions where the activity of dissolved H_2 is controlled by equilibration of the fluid with the pyrite-pyrrhotite-magnetite (PPM) mineral assemblage according to the reaction

$$\underset{\text{pyrite}}{3FeS_2} + \underset{\text{magnetite}}{Fe_3O_4} + 4H_{2(aq)} = \underset{\text{pyrrhotite}}{6FeS} + 4H_2O. \quad (18)$$

For H_2 = 50 mmolal, calculated values of $t_{1/2}$ are 376 yr at 100°C, 7.8 yr at 150°C, 0.4 yr at 200°C, and 0.03 yr at 250°C. For equilibrium with PPM, calculated half-lives are ~1 million, 6500, 124, and 4.6 yr at 100, 150, 200, and 250°C, respectively. Although these calculations are subject to large uncertainties, the calculated half-lives suggest that the reduction of ΣCO_2 to Σformate is rapid on geologic time scales at temperatures as low as 100°C. Of course, these half-lives would only apply to situations where the ΣCO_2 is initially far from equilibrium with respect to Σformate and H_2.

4.3. Metastable Thermodynamic Equilibrium Between ΣCO_2 and Σformate

During this study, all of the experiments conducted at temperatures of 225°C and above rapidly approached $\Sigma CO_2/\Sigma$formate ratios consistent with thermodynamic equilibrium. This was observed whether the initial disturbance of the chemical system resulted in an excess of ΣCO_2 or Σformate. Equilibrium between ΣCO_2 and Σformate in this case is metastable, because nearly all of the carbon in the experiments would have been converted to CH_4 if stable thermodynamic equilibrium had been achieved at the reducing conditions of the experiments. However, CH_4 remained far out of equilibrium with ΣCO_2 and

Σformate in all experiments, reflecting strong kinetic inhibitions for reduction of these compounds to CH_4. Ratios of ΣCO_2 to Σformate also progressed towards, but did not attain, equilibrium values in the NiFe experiment at 175 and 177°C after reacting for up 1050 h following injection of $NaHCO_3$ or formic acid. The progress of these systems towards equilibrium suggests that they were likely to have equilibrated at these lower temperatures if the experiments had been allowed to continue for a more extended period.

In contrast to the other results, no detectable progress towards equilibrium was observed in the olivine experiment at 175°C even though thermodynamic calculations indicated that ΣCO_2 and Σformate remained far from equilibrium (Fig. 7). The rapid attainment of equilibrium between ΣCO_2 and Σformate in the olivine experiment at 250°C and in a similar experiment at 300°C reported by McCollom and Seewald (2001) suggests that there is nothing inherent to the olivine experiment that would have prevented reactions toward equilibrium from moving forward. This experiment may have been moving towards equilibrium at a rate that was too slow to be detectable on the time scale of our study.

4.4. Formation of Hydrocarbons by Reduction of Dissolved CO_2

In each of the experiments in this study, the strongly reducing conditions present in the reaction vessels thermodynamically favored the production of methane and other hydrocarbons from the reduction of CO_2. However, isotopic analyses indicated that, except for a small amount of methane produced in the NiFe experiment at 260°C between 1171 and 3257 h, none of the trace amounts of hydrocarbons observed during the experiments showed any evidence for a contribution from the injected ^{13}C-labeled carbon sources. This observation strongly indicates that, aside from the methane generated in the NiFe experiment, there was no production of hydrocarbons from reduction of ΣCO_2 or formate in the experiments and reactions to form these compounds were kinetically inhibited at the experimental conditions.

In a recent study, Horita and Berndt (1999) reported the reduction of aqueous ΣCO_2 to CH_4 using a NiFe-alloy catalyst. They observed $>$ 90% conversion of $\sim$12 mmol kg^{-1} ΣCO_2 to CH_4 in $<$ 340 h at 300°C and $>$45% conversion after 2173 h at 200°C. In addition, they reported an increase in conversion rates with increasing mass of NiFe alloy. Although the alloy in our NiFe experiment had a similar composition (2–9 wt.% Fe) to that of Horita and Berndt (1999) and was present in much greater amounts, we observed substantially slower conversion of ΣCO_2 to CH_4 ($<$1% conversion of $\sim$230 mmol kg^{-1} ΣCO_2 in $>$ 2000 h at 260°C). Since Horita and Berndt (1999) reported that the effectiveness of their NiFe alloy catalyst decreased rapidly over time during heating, this discrepancy may reflect a loss of catalytic ability of NiFe alloy in our experiment during extended heating, especially since the alloy in our experiment was heated with H_2O for an extended period before introduction of a CO_2 source. Indeed, CH_4 production in the NiFe experiment ceased altogether after 3257 h.

5. IMPLICATIONS FOR THE GEOCHEMISTRY OF NATURAL SYSTEMS

5.1. Controls on the Abundance of Formate

Our results indicate that chemical equilibrium with dissolved CO_2 at the prevailing oxidation state and pH of the system is likely to control the abundance of dissolved Σformate in many geologic fluids in subsurface and hydrothermal environments. As noted above, formate is usually found at much lower concentrations than acetate and propionate in oil-field brines and formation waters from sedimentary basins, but occurs at concentrations comparable to, or greater than, acetate and propionate in hydrothermal fluids, pore fluids from serpentinites, and the aqueous products of hydrous pyrolysis of kerogens in some laboratory experiments (e.g., Haggerty, 1991; Haggerty and Fisher, 1992; Shebl and Surdam, 1996; Amend et al., 1998; Zeng and Liu, 2001). In the past, the low relative concentrations of formate in sedimentary basins have been interpreted to reflect rapid decomposition of formate compared with other organic acids. Conversely, the high concentrations of formate in other fluids have been attributed to sampling soon after the organic acids had formed and before they had time to decompose to any appreciable extent (Haggerty, 1991; Bell and Palmer, 1994). Our results suggest that the higher relative concentrations of formate in some fluids is more likely attributable to the greater thermodynamic stability of formate in those environments than a reflection of reaction kinetics.

Particularly high concentrations of formate have been observed in pore fluids from seamount-forming serpentinite diapirs on the ocean floor (Haggerty, 1991; Haggerty and Fisher, 1992). Acetate occurred at much lower concentrations in the same fluids, and propionate was below detection limits. Although Haggerty (1991) suggested that the high concentrations of formate in the pore fluids were derived from thermal decomposition of bioorganic matter entrained from nearby sediments, reduction of CO_2 within the serpentinites appears to be a more feasible source for formate. Given the strongly reducing conditions and alkaline pH that develop during hydrothermal alteration of olivine (e.g., Table 3; McCollom and Seewald, 2001), high concentrations of formate would be expected at equilibrium with CO_2 in serpentinized olivine-rich ultramafic rocks.

Indeed, reduction of CO_2 during serpentinization may represent a substantial source of formate for the oceans, where it could support the growth of microorganisms at and below the seafloor. Serpentinized peridotites are widespread on the ocean floor where they may make up as much as 20% of the basement rocks exposed along spreading ridges and transform faults (Charlou and Donval, 1993; Cannat et al., 1995; Früh-Green et al., 1996; Mével and Stamoudi, 1996). Methane-rich hydrothermal fluids have been observed venting from several of these serpentinites (e.g., Charlou et al., 1998; Kelley et al., 2001). It is likely that a substantial fraction of the CO_2 in hydrothermal fluids circulating through these rocks may be converted to formate and released to the ocean. To date, however, the concentration of formate in fluids venting from serpentinites on the seafloor has not been reported.

Much lower concentrations of formate are predicted at equilibrium in sedimentary basin fluids where conditions tend to be much less reducing. For instance, Helgeson et al. (1993) esti-

mate that a family of oil-field waters from the Texas Gulf Coast at ~100 to 160°C have in situ pHs in the range of 5.5 to 6.5 and oxidation states that are consistent with buffering by the mineral assemblage pyrite + pyrrhotite + magnetite (PPM) (Eqn. 18). For H_2 buffered by the PPM assemblage according to Eqn. 18 and ΣCO_2 in the fluids of ~4.4 to 12.1 mmol/L (Carothers and Kharaka, 1978), calculated equilibrium concentrations of formate in the oil-field waters are in the range of 0.005 to 0.076 mmol kg^{-1}. For comparison, acetate concentrations in the oil-field waters range from 0.9 to 23.5 mmol/L (Carothers and Kharaka, 1978). Although the concentrations of formate were not reported in the Texas oil-field waters, the small concentrations predicted for equilibrium are consistent with the trace amounts of formate and high acetate/formate ratios reported in oil-field waters from other locations (e.g., Fisher and Boles, 1990; MacGowan and Surdam, 1990; Barth, 1991).

The apparent equilibration of ΣCO_2 and Σformate in geologic fluids has a potential practical application in monitoring the oxidation state of subsurface geochemical environments. Although many geochemical reactions, both inorganic and organic, in subsurface environments are sensitive to oxidation state, this is often a particularly difficult parameter to measure. In the reducing conditions found in most subsurface aqueous environments, the concentration of H_2 is a good indicator of oxidation state since the low oxygen fugacities mean that O_2 is usually below detectable limits. However, measurement of the concentration of H_2 is often not possible owing the difficulties in quantitative sampling of volatile species. In these environments, indirect methods generally have to be employed to estimate the oxidation state (e.g., Helgeson et al., 1993). Since the equilibrium between ΣCO_2 and Σformate is sensitive to the concentration of H_2, accurate estimates of H_2 concentration can be made from measured concentrations of ΣCO_2 and Σformate together with fluid pH and temperature. Such estimates could be useful in interpreting the oxidation state of geologic fluids such as those found in petroleum reservoirs, sedimentary basins, and geothermal systems.

5.2. Formation of Abiotic Hydrocarbons

Methane and other hydrocarbons with an apparent abiotic origin have been observed in a variety of geologic environments, including serpentinites, crystalline igneous rocks from continental and oceanic crust, and hydrothermal fluids venting on the ocean floor (e.g., Abrajano et al., 1988; Welhan, 1988; Sherwood Lollar et al., 1993, 2002; Salvi and Williams-Jones, 1997; Charlou et al., 1998; Kelley and Früh-Green, 1999; Normand and Williams-Jones, 1999; Kelley et al., 2001). A frequently invoked scenario for the formation of these compounds involves the reduction of CO_2 by the Fischer-Tropsch process or a related mechanism, with H_2 produced by reaction of water with olivine or other ferrous iron-bearing minerals serving as the reductant. In addition, it has recently been proposed that formate may be a reaction intermediate in the formation of methane and more complex hydrocarbons from reduction of CO_2 (Horita and Berndt, 1999; Schoonen et al., 1999).

Experimental support for this scenario was apparently supplied by Berndt et al. (1996), who observed production of methane, ethane, and propane during hydrothermal serpentinization of olivine in laboratory experiments and inferred that these compounds were produced by reduction of dissolved CO_2. However, a subsequent study using ^{13}C-labeled carbon sources has shown that, except for a small amount of methane, the hydrocarbons generated during hydrothermal alteration of olivine in laboratory experiments are derived from background sources rather than reduction of CO_2 (McCollom and Seewald, 2001). The lack of hydrocarbon generation in the present experiments provides additional evidence that the products of aqueous CO_2 reduction during serpentinization of olivine may be limited to small amounts of methane.

Despite the strongly reducing conditions, presence of potential catalysts, and high concentrations of formate in the experiments, no organic compounds more complex than methane were generated. These results are in sharp contrast to the rapid formation of organic products, including linear alkanes, alkanols, and alkanoic acids to $> C_{20}$, observed when aqueous solutions of formic acid are heated in fixed-volume reactors with a gas phase present (McCollom et al., 1999). These contrasting results suggest that a gas phase may be necessary for the formation of complex hydrocarbons under hydrothermal conditions, perhaps because the presence of a liquid water may interfere with the formation of C–C bonds on the catalyst's surface. In this respect, it should be noted that the Fischer-Tropsch process is typically a gas phase reaction, and, although the reaction has been shown to proceed in the presence of water vapor, it has apparently never been demonstrated that the Fischer-Tropsch reaction can proceed in a liquid aqueous environment.

If further research confirms this hypothesis, it will greatly limit the range of geologic environments where abiotic synthesis can occur. For instance, one environment where continuous synthesis of organic compounds is thought to occur is basalt-hosted hydrothermal systems along midocean ridges (Holm, 1992; Shock and Schulte, 1998). However, if a gas phase is required for the process, organic compounds may be generated only in those parts of the systems where conditions are appropriate for formation of a vapor phase. Similarly, occurrences of abiotic hydrocarbons in crystalline igneous rocks may indicate that a gas phase was present at the time of their formation (e.g., Normand and Williams-Jones, 1999).

6. CONCLUSIONS

While the abundances of other aqueous organic acid and acid anions in geologic systems appear to be controlled primarily by kinetic factors, the results of this study indicate that thermodynamic equilibrium with CO_2 and H_2 will exert a predominant influence on the abundance of formic acid and formate in most high temperature (>100°C) geologic environments. Minerals appear to have little effect on the stability of formate and formic acid, except through their influence on pH and concentration of CO_2. Reduction of aqueous CO_2 during hydrothermal alteration of Fe(II)-bearing minerals such as olivine may be a significant source of formate in some geologic environments, but further reduction and polymerization of carbon to form complex hydrocarbons appears to be inhibited under aqueous conditions.

Acknowledgments—The authors greatly appreciate the helpful comments of Laura Crossey, Jeremy Fein, Tom Giordano, and an anony-

mous reviewer on the initial version of the manuscript. This research was supported by NSF Earth Sciences grant EAR-0073850 (T.M.M.) and DOE grant DE-FG02-97ER14746 (J.S.S.).

Associate editor: J. B. Fein

REFERENCES

Abrajano T. A., Sturchio N. C., Bohlke J. K., Lyon G. L., Poreda R. J., and Stevens C. M. (1988) Methane-hydrogen gas seeps, Zambales Ophiolite, Philippines: Deep or shallow origin? *Chem. Geol.* **71,** 211–222.

Akiya N. and Savage P. E. (1998) Role of water in formic acid decomposition. *AIChE J.* **44,** 405–415.

Amend J. P., Amend A. C., and Valenza M. (1998) Determination of volatile fatty acids in the hot springs of Volcano, Aeolian Islands, Italy. *Org. Geochem.* **28,** 699–705.

Barth T. (1991) Organic acids and inorganic ions in waters from petroleum reservoirs, Norwegian continental shelf: A multivariate statistical analysis and comparison with American reservoir formation waters. *Appl. Geochem.* **6,** 1–15.

Bell J. L. S. and Palmer D. A. (1994) Experimental studies of organic acid decomposition. In *Organic Acids in Geological Processes* (eds. E. D. Pittman and M. D. Lewan), pp. 227–269. Springer-Verlag, Berlin, Germany.

Bell J. S., Palmer D. A., Barnes H. L., and Drummond S. E. (1994) Thermal decomposition of acetate: III. Catalysis by mineral surfaces. *Geochim. Cosmochim. Acta* **58,** 4155–4177.

Berndt M. E., Allen D. E., and Seyfried W. E. Jr. (1996) Reduction of CO_2 during serpentinization of olivine at 300°C and 350 bar. *Geology* **24,** 351–354.

Bjerre A. B. and Sørensen E. (1992) Thermal decomposition of dilute aqueous formic acid solutions. *Ind. Eng. Chem. Res.* **31,** 1574–1577.

Cannat M., Mével C., Maia M., Deplus C., Durand C., Gente P., Agrinier P., Belarouchi A., Dubuisson G., Humler E., and Reynolds J. (1995) Thin crust, ultramafic exposures, and rugged faulting patterns at the Mid-Atlantic Ridge (22°-24°N). *Geology* **23,** 49–52.

Carothers W. W. and Kharaka Y. K. (1978) Aliphatic acid anions in oil-field waters- Implications for origin of natural gas. *Am. Assoc. Petrol. Geol. Bull.* **62,** 2441–2453.

Charlou J.-L. and Donval J. P. (1993) Hydrothermal methane venting between 12°N and 26°N along the Mid-Atlantic Ridge. *J. Geophys. Res.* **98,** 9625–9642.

Charlou J.-L., Fouquet Y., Bougault H., Donval J. P., Etoubleau J., Jean-Baptiste P., Dapoigny A., Appriou P., and Rona P. A. (1998) Intense CH_4 plumes generated by serpentinization of ultramafic rocks at the intersection of the 15°20′N fracture zone and the Mid-Atlantic Ridge. *Geochim. Cosmochim. Acta* **62,** 2323–2333.

Chen Q. W. and Bahnemann D. W. (2000) Reduction of carbon dioxide by magnetite: Implications for the primordial synthesis of organic molecules. *J. Am. Chem. Soc.* **122,** 970–971.

Crossey L. J. (1991) Thermal degradation of aqueous oxalate species. *Geochim. Cosmochim. Acta* **55,** 1515–1527.

Fisher J. B. and Boles J. R. (1990) Water-rock interaction in Tertiary sandstones, San Joaquin basin, California, U. S. A.: Diagenetic controls on water composition. *Chem. Geol.* **82,** 83–101.

Früh-Green G. L., Ples A., and Lécuyer C. (1996) Petrologic and stable isotope constraints on hydrothermal alteration and serpentinization of the EPR shallow mantle at Hess Deep (Site 895). *Proc. Ocean Drill. Prog. Sci. Results* **147,** 255–291.

Haggerty J. A. (1991) Evidence from fluid seeps atop serpentine seamounts in the Mariana Forearc: Clues for emplacement of the seamounts and their relationship to forearc tectonics. *Mar. Geol.* **102,** 293–309.

Haggerty J. A. and Fisher J. B. (1992) Short-chain organic acids in interstitial waters for Mariana and Bonin Forearc serpentines: Leg 125. *Proc. Ocean Drill. Prog. Sci. Results* **125,** 387–395.

Helgeson H. C., Knox A. M., Owens C. E., and Shock E. L. (1993) Petroleum, oil filed waters, and authigenic mineral assemblages: Are they in metastable equilibrium in hydrocarbon reservoirs? *Geochim. Cosmochim. Acta* **57,** 3295–3339.

Holm N. G., ed. (1992) *Marine Hydrothermal Systems and the Origin of Life*. Kluwer, Dordrecht, the Netherlands.

Horita J. and Berndt M. E. (1999) Abiogenic methane formation and isotopic fractionation under hydrothermal conditions. *Science* **285,** 1055–1057.

Johnson J. W., Oelkers E. H., and Helgeson H. C. (1992) SUPCRT92: A software package for calculating the standard molal thermodynamic properties of minerals, gases, aqueous species, and reactions from 1 to 5000 bar and 0 to 1000°C. *Comput. Geosci.* **18,** 899–947.

Kawamura K. and Nissenbaum A. (1992) High abundance of low molecular weight organic acids in hypersaline spring water associated with a salt daipir. *Org. Geochem.* **18,** 469–476.

Kelley D. S. and Früh-Green G. L. (1999) Abiogenic methane in deep-seated mid-ocean ridge environments: Insights from stable isotope analyses. *J. Geophys. Res.* **104,** 10439–10460.

Kelley D. S., Karston J. A., Blackman D. K., et al. (2001) An off-axis hydrothermal vent field near the Mid-Atlantic Ridge at 30° N. *Nature* **412,** 145–149.

Kharaka Y. K., Lundegard P. D., Ambats G., Evans W. C., and Bischoff J. L. (1993) Generation of aliphatic acid anions and carbon dioxide by hydrous pyrolysis of crude oils. *Appl. Geochem.* **8,** 317–324.

Lundegard P. D. and Sentfle J. T. (1987) Hydrous pyrolysis: A tool for the study of organic acid synthesis. *Appl. Geochem.* **2,** 605–612.

MacGowan D. B. and Surdam R. C. (1990) Carboxylic acids and anions in formation waters, San Joaquin Basin and Louisiana Gulf Coast, U. S. A.: Implications for clastic diagenesis. *Appl. Geochem.* **5,** 687–701.

Maiella P. G. and Brill T. B. (1998) Spectroscopy of hydrothermal reactions. 10. Evidence of wall effects in decarboxylation kinetics of 1.00 m HCO_2X (X=H, Na) at 280-330°C and 275 bar. *J. Phys. Chem. A* **102,** 5886–5891.

Martens C. (1990) Generation of short-chain organic acid anions in hydrothermally altered sediments of the Guaymas Basin, Gulf of California. *Appl. Geochem.* **5,** 71–76.

McCollom T. M. and Seewald J. S. (2001) A reassessment of the potential for reduction of dissolved CO_2 to hydrocarbons during serpentinization of olivine. *Geochim. Cosmochim. Acta* **65,** 3769–3778.

McCollom T. M. and Seewald J. S. (2003) Experimental study of the hydrothermal reactivity of organic acids and acid anions: II. Acetic acid, acetate, and valeric acid. *Geochim. Cosmochim. Acta* **67,** 0000–0000.

McCollom T. M., Ritter G., and Simoneit B. R. T. (1999) Lipid synthesis under hydrothermal conditions by Fischer-Tropsch-type reactions. *Orig. Life Evol. Biosphere* **29,** 153–166.

Mével C. and Stamoudi C. (1996) Hydrothermal alteration of the upper-mantle section at Hess Deep. *Proc. Ocean Drill. Prog. Sci. Results* **147,** 293–309.

Normand C. and Williams-Jones A. E. (1999) Hydrocarbon speciation in carbon-oxygen-hydrogen fluids during serpentinization [abstract]. In *Ninth Ann. V. M. Goldschmidt Conference*, 210.

Palmer D. A. and Drummond S. E. (1986) Thermal decarboxylation of acetate. Part I. The kinetics and mechanism of reaction in aqueous solution. *Geochim. Cosmochim. Acta* **50,** 813–823.

Pittman E. D. and Lewan M. D., eds. (1994) *Organic Acids in Geological Processes.* Springer-Verlag, Berlin, Germany.

Salvi S. and Williams-Jones A. E. (1997) Fischer-Tropsch synthesis of hydrocarbons during sub-solidus alteration of the Strange Lake peralkaline granite, Quebec/Labrador, Canada. *Geochim. Cosmochim. Acta* **61,** 83–99.

Satterfield C. N., Hanlon R. T., Tung S. E., Zou Z., and Papaefthymiou G. C. (1986) Effect of water on the iron-catalyzed Fischer-Tropsch synthesis. *Ind. Eng. Chem. Prod. Res. Dev.* **25,** 4074–414.

Schoonen M. A. A., Xu Y., and Bebie J. (1999) Energetics and kinetics of the prebiotic synthesis of simple organic acids and amino acids with the FeS-H_2S/FeS_2 redox couple as reductant. *Orig. Life Evol. Biosphere* **29,** 5–32.

Seyfried W. E. Jr., Janecky D. R., and Berndt M. E. (1987) Rocking autoclaves for hydrothermal experiments, II. The flexible reaction-cell system. In *Hydrothermal Experimental Techniques* (eds. G. C. Ulmer and H. L. Barnes) pp. 216–239. John Wiley, New York.

Shebl M. A. and Surdam R. C. (1996) Redox reactions in hydrocarbon clastic reservoirs: Experimental validation of this mechanism for porosity enhancement. *Chem. Geol.* **132,** 103–117.

Sherwood Lollar B., Frape S. K., Weise S. M., Fritz P., Macko S. A., and Welhan J.A. (1993) Abiogenic methanogenesis in crystalline rocks. *Geochim. Cosmochim. Acta* **57,** 5087–5097.

Sherwood Lollar B., Westgate T. D., Ward J. A., Slater G. F., and Lacrampe-Couloume G. (2002) Abiogenic formation of alkanes in the Earth's crust as a minor source for global hydrocarbon reservoirs. *Nature* **416,** 522–524.

Shock E. L. (1995) Organic acids in hydrothermal solutions: Standard molal thermodynamic properties of carboxylic acids and estimates of dissociation constants at high temperatures and pressures. *Am. J. Sci.* **295,** 496–580.

Shock E. L. and Schulte M. D. (1998) Organic synthesis during fluid mixing in hydrothermal systems. *J. Geophys. Res.* **103,** 28513–28517.

Small J. S. and Manning D. A. C. (1993) Laboratory reproduction of morphological variation in petroleum reservoir clays: Monitoring of fluid composition during illite precipitation. In *Geochemistry of Clay-Pore Fluid Interactions* (eds. D. A. C. Manning, P. L. Hall, and C. R. Hughes), pp. 181–212. Chapman & Hall, London.

Welhan J. A. (1988) Origins of methane in hydrothermal systems. *Chem. Geol.* **71,** 183–198.

Wolery T. J. (1992) *EQ3NR, a Computer Program for Geochemical Aqueous Speciation-Solubility Calculations: Theoretical Manual, User's Guide, and Related Documentation (version 7.0)*. Lawrence Livermore National Laboratory, Livermore, CA.

Yu J. and Savage P. E. (1998) Decomposition of formic acid under hydrothermal conditions. *Ind. Eng. Chem. Res.* **37,** 2–10.

Zeng Y. and Liu J. (2000) Short-chain carboxylates in fluid inclusions in minerals. *Appl. Geochem.* **15,** 13–25.